



Escola d'Enginyeria de Telecomunicació i
Aeroespacial de Castelldefels

UNIVERSITAT POLITÈCNICA DE CATALUNYA

TREBALL DE FI DE CARRERA

TÍTOL DEL TFC: Study of a Coke Can as a rocket structure and its flutter effects

TITULACIÓ: Enginyeria Tècnica Aeronàutica, especialitat Aeronavegació

AUTORS: Pau Manyà Saez i Daniel Gómez Sañé

DIRECTOR: Joshua Tristancho Martínez

CODIRECTOR: Jordi Gutiérrez Cabello

DATA: 10 de Maig de 2013

Títol: Study of a Coke Can as a rocket structure and its flutter effects

Autors: Pau Manyà Saez and Daniel Gómez Sañé

Director: Joshua Tristancho Martínez

Codirector: Jordi Gutiérrez Cabello

Data: 10 de Maig de 2013

Resum

Aquest treball final de carrera (TFC) és un estudi de les propietats d'una llauna de refresc per ser reutilitzada com estructura per a un coet. El treball se centra en els possibles efectes de fluctuació que aquesta estructura podria presentar.

Es compon de dos grans blocs: El primer bloc és un bon model de l'estructura proposada. El segon bloc és un bon model intern del flux en el coet. Per aquesta raó, es requereixen dos estudiants.

El primer bloc estudia una llauna de Coca Cola tipus i el seu comportament quant a punts febles estructurals (Propagació d'esquerdes, brides i tancament). Es realitzen algunes proves de pressió. A causa de que aquesta estructura tindrà una càrrega tèrmica molt alta, es realitza un estudi del material, que és acer. A més es té en compte el combustible sòlid (APCP o Candy) que porti dins de l'estructura del coet.

El segon estudi estudia el flux a l'interior de la cambra de combustió a fi de trobar punts febles, camp de pressions, camps de temperatures i el camp de velocitats. També s'estudia el comportament del flux en la gola. Es realitzen algunes simulacions de SolidWorks calculades en termes de dinàmica de fluids (CFD). A més, s'estudia el comportament elàstic de l'estructura i els modes d'oscil·lació. Finalment s'esbrina si el flux generarà freqüències de ressonància que es trobin en el rang dels modes d'oscil·lació estructurals.

Paraules clau:

Aleteig, coet, llauna, ressonància, modes d'oscil·lació, Computed Fluid Dynamics

Title: Study of a Coke Can as a rocket structure and its flutter effects
Authors: Pau Manyà Saez i Daniel Gómez Sañé
Director: Joshua Tristancho Martínez
Codirector: Jordi Gutiérrez Cabello
Date: May, 10th 2013

Overview

This final bachelor work (TFC) is a study of Coke Can properties to be reused in a rocket as a structure. The work is focused in the possible flutter effects that this structure could present.

There are two main blocks to achieve: First block is a good proposed structure model. Second block is a good internal rocket flow model. For this reason, two students are required.

First block studies the Coke Can behaviour in terms of weak structural points (Crack propagation, flanges, and bulkhead). Some pressure test will be done. Because this structure will have a very high thermal load, the steel material study is required. In addition, the solid propellant (APCP or Candy) inside the rocket structure should be taken into account.

Second block studies the flow inside the combustion chamber in order to find weak points, the pressure field, the temperature field and speed field. Also it is required to know the flow behaviour in the nozzle. Some SolidWorks simulations in terms of Computed Fluid Dynamics (CFD) should be done. In addition, structural elastic studies will provide the oscillation modes. It is necessary to know if the flow will generate resonant frequencies that are in the range of the structural oscillation modes.

Keywords:

Flutter, Rocket, Coke Can, Resonance, Oscillation modes, Computed Fluid Dynamic

INDEX

ACRONYMS, ABBREVIATIONS AND DEFINITIONS	12
INTRODUCTION.....	13
CHAPTER 1. STATE OF THE ART	15
1.1 How does a rocket works	15
1.1.1 Hercules – Space shuttle booster	17
1.1.2 P230 – Ariane 5 booster.....	17
1.1.3 Star37 – FLTSTACOM satellite	17
1.1.4 LGM-30 – Minuteman ICBM.....	17
1.1.5 Summary of the technical parameters.....	17
1.2 WikiLauncher	18
CHAPTER 2. ENGINE STRUCTURE VALIDATION.....	19
2.1 Structure selection and mechanical study	19
2.1.1 Soda Can manufacturing.....	20
2.1.2 Soda Can integration.....	20
2.1.3 Mechanical properties study.....	20
2.1.4 Summary of pressure tests.....	24
2.2 Structure thermal load study.....	24
2.2.1 Combustion chamber pressure simulation	24
2.2.2 Combustion chamber pressure estimation.....	26
2.3 Propellant study and selection	27
2.3.1 Black powder propellants	27
2.3.2 Zinc-sulfur propellants	27
2.3.3 Candy propellants.....	27
2.3.4 Double-based propellants.....	27
2.3.5 Composite propellants.....	28
2.3.6 Propellant selection	28
CHAPTER 3. NOZZLE DESIGN AND VALIDATION.....	29
3.1 Design parameters	29
3.1.1 Burn rate.....	29
3.1.2 Mass flow.....	30
3.1.3 Throat diameter	31
3.1.4 Velocity of the exhaust	33
3.1.5 Nozzle efficiency.....	33
3.1.6 Burning time.....	34
3.1.7 Thrust.....	34
3.1.8 DeltaV	35
3.2 Nozzle design.....	35
3.2.1 Main parameters.....	35
3.2.1 Drawings.....	35
3.2.2 Construction parameters	37
3.3 Burn type study and selection	38

3.4	Performance calculation	39
3.5	Nozzle validation.....	40
CHAPTER 4. ENGINE TEST		43
4.1	Flutter test	43
4.2	Oscillation modes.....	43
4.2.1	Early tests	43
4.2.2	Oscillation modes	44
4.3	Stage1 Burn03rd Test	46
4.3.1	Test 03 setup	46
4.3.2	Results.....	46
4.4	Stage1 Burn04th Test.....	46
4.4.1	Test 04 setup	46
4.4.2	Results.....	47
4.5	Stage1 Burn05th Test.....	47
4.5.1	Test 05 setup	47
4.5.2	Results.....	47
4.6	Stage1 Burn06th Test.....	48
4.6.1	Test 06 setup	48
4.6.2	Results.....	48
4.7	Stage1 Burn07th Test.....	49
4.7.1	Test 07 setup	49
4.7.2	Results.....	49
4.8	Stage1 Burn08th Test.....	49
4.8.1	Test 08 setup	49
4.8.2	Results.....	50
4.9	Stage1 Burn09rd Test	50
4.9.1	Test 09 setup	50
4.9.2	Results.....	50
4.10	Stage1 Burn tests summary	52
CHAPTER 5. CONCLUSIONS.....		53
5.1	Conclusions	53
5.2	Future work	53
5.3	Environmental impact	54
CHAPTER 6. BIBLIOGRAPHY.....		55

LIST OF FIGURES

Figure 1 – Delivered Specific Impulse evolution.....	16
Figure 2 – (a) Max pressure vs Mass and (b) Crack propagation.....	22
Figure 3 – (a) Deformations, (b) Relative to the original shape and (c) Real case	25
Figure 4 – Propellant grain dimensions	31
Figure 5 – Draft of main nozzle parameters	35
Figure 6 – 3D model for the bottle and the nozzle.....	36
Figure 7 – Detailed nozzle parameters (I)	36
Figure 8 – Detailed nozzle parameters (II)	36
Figure 9 – Detailed nozzle parameters (III)	37
Figure 10 – Detailed bottle parameters	37
Figure 11 – Thrust vs time for each case	38
Figure 12 – Thrust vs time for the optimum case	40
Figure 13 – Pressure vs time for the optimum case	40
Figure 14 – Burn rate vs time for the optimum case.....	40
Figure 15 – Comparing real flame vs simulated flame	41
Figure 16 – CFDs for pressure, temperature and Mach number velocity	42
Figure 17 – Preheating and oscillation modes number 7, 8 and 9.....	45
Figure 18 – Stage1 Burn03rd pictures.....	46
Figure 19 – Stage1 Burn04th pictures.....	47
Figure 20 – Stage1 Burn05th pictures.....	48
Figure 21 – Stage1 Burn06th pictures.....	48
Figure 22 – Stage1 Burn07th pictures.....	49
Figure 23 – Stage1 Burn08th pictures.....	50
Figure 24 – Stage1 Burn09th pictures.....	51

LIST OF TABLES

Table 1 – Solid propellant rocket technical parameters summary	18
Table 2 – Physical parameters and maximum pressure for each vessel.....	19
Table 3 – Physical parameters and maximum pressure for each vessel.....	21
Table 4 - Drag summary from previous sections.....	24
Table 5 - Summary for various cases of simulation series	38
Table 6 - Summary for stage1 burn tests	52

Agradecimientos

Pau Manyà agradece al tutor de nuestro trabajo Joshua Tristancho el tiempo dedicado a nosotros y a nuestro trabajo. Gracias a su empuje ha resultado más atractivo. Por supuesto también a mi compañero Daniel por las horas dedicadas. A Pau Sendra, Elliot Morales y Jordi Tudela por dedicar parte de su tiempo a enseñarnos a manejar algunos softwares empleados en el trabajo. Finalmente agradecer a mis padres que me dejaron el coche para llegar a la facultad de forma más rápida.

Daniel Gómez agradece a Joshua Tristancho por su paciencia y esfuerzo para hacer este trabajo más apetecible y ser uno más del equipo.

Gracias a mi compañero Pau por su gran dedicación a este trabajo.

Gracias a Jordi Tudela por su ayuda con las simulaciones con ANSYS, que tanto han aportado a este trabajo.

Y por último, pero no menos importante, gracias al señor de conserjería que me abrió la puerta del aula de informática para que pudiese hacer las simulaciones.

Trademarks

- ANSYS
- Coca Cola
- Discovery Channel
- SolidWorks
- YouTube

ACRONYMS, ABBREVIATIONS AND DEFINITIONS

AN	Ammonium Nitrate
ANSYS	Analysis Systems
AoA	Angle of Attack
AP	Ammonium Perchlorate
APCP	Ammonium Perchlorate Composite Propellant
CFD	Computed Fluid Dynamics
COTS	Commercial Off-The-Shelf
ESA	European Space Agency
GTO	Geostationary Transfer Orbit
LEO	Low Earth Orbit
NASA	National Aeronautics and Space Administration
UHF	Ultra High Frequency

INTRODUCTION

The technologic goal is to get a cheap engine, made with easy to achieve materials and a simple design. That is why the engine must be a solid propellant engine, based on a container which has to be resistant enough to certain temperature and pressure conditions. With this kind of engine it will be possible to make launchings that will be able to put into orbit small satellites with low costs while respecting the environment.

The solution is to look for available components in the domestic market (COTS) to reduce costs while being in the state of art. The engine size will depend on the chosen COTS components. In our case, we will propose to use a Soda Can. It will be required to know the Soda Can limitations in order to take them into account in the nozzle design. It will be started off from some engine running parameters related to the propellant thermal properties and the rocket trajectory. CFD simulations will be done in order to design and build an efficient nozzle. Finally, some engine prototype will be implemented to compare the actual results with the simulation results.

Chapter 1 has the state of the art about solid propellant engines, basic theory and an introduction to the WikiLauncher.

Chapter 2 has the engine structure study and validation.

Chapter 3 has the nozzle design and validation that depends on the grain burn type. Some trajectory simulations are run in order to compare different nozzles and burner types. In addition, some computing-aided fluid dynamics (CFD) simulations are done in order to compare with real nozzle flames.

Chapter 4 addresses the flutter effects and vibration modes. Then a series of real burn tests were performed in order to have real data and it will be compared with simulations. Finally a summary of main parameters for each burn is presented.

Chapter 5 has the conclusions, future work and environmental impact.

Chapter 6 has the bibliography and the annexes after that.

CHAPTER 1. STATE OF THE ART

Solid propellant rocket engines and liquid propellant rocket engines obtain the thrust in the same way: They convert enthalpy¹ to kinetic energy. Because of this thermodynamic similitude, there will be the same design restrictions on both the nozzle and the combustion chamber.

The main difference between solid propellant rockets and liquid ones is that in solid propellant rockets have the grains, which is the solid compound that results from mixing the oxidizer and the fuel before launch. This propellant is casted into the combustion chamber and embedded to the nozzle. The thrust is obtained when the inner surface of the grain is ignited, and it is continuously obtaining the thrust until the burning is finished. So there is no propellant tanks separated from combustion chamber in solid propellant rockets. The absence of these propellant tanks makes the design much simpler, so it enables a considerable number of applications.

Even though a high exhaust velocity cannot be reached, this simplicity produce a low cost, a high mass ratio and reliability. Several kinds of solid propellants are detailed on section 2.3 Propellant study and selection.

The WikiSat satellite is being designed to fit **N-Prize**² contest rules, it is a femto-satellite with less than 20 grams of mass. The payload is able to take over control of the launcher and assume autonomous decisions if needed. The most restrictive parameter to fulfill the rules is the cost. That's why we decided to implement our non-redundancy policy, so we use Single Fault Tolerant systems.

Early studies showed that it will be able to carry a 20 grams payload to 250 km altitude for a few days, if we have a 1.5 m length and 35 kg launcher. The combustible used will be Ammonium Perchlorate Composite Propellant (APCP). Also, performances could be improved if a initial stage is added that consists of a balloon and a launching ramp.

1.1 How does a rocket works

A rocket is a spacecraft that obtains thrust by the reaction of the expulsion of combustion gases from the rocket motor. These gases are generated by the combustion of solid or liquid propellant in a high pressure combustion chamber. This fluid passes through a supersonic nozzle that uses the calorific energy in order to accelerate it. The high velocity that the fluid achieves at the nozzle exit allows the rocket to obtain a reaction force by Third Newton's Law.

The Tsiolkovski equation (1.1) considers the rocket motion principle:

¹ **Enthalpy** is a measure of the total energy of a thermodynamic system. It includes the internal energy, which is the energy required to create a system, and the amount of energy required to make room for it by displacing its environment and establishing its volume and pressure. (Source: Wikipedia)

² <http://www.n-prize.com>

$$\Delta v = v_e \ln \frac{m_0}{m_1} \quad (1.1)$$

where m_0 is the initial total mass (including propellant), m_1 is the final total mass, v_e is the effective exhaust velocity and Δv is the maximum change of speed of the rocket. If the exhaust velocity is not high or the structure is too heavy the rocket will not achieve a large delta-v and therefore, there will not be an important change of speed. This increment in velocity is assumed to be instantaneously but later simulations will show that slow burns degrades the specific impulse due to this fact.

Solid propellant rockets were introduced by the Chinese (early 13th century). They were propelled by black powder and their specific impulse was below 100 s. There were no events occurred until late 17th and 18th when nitro-cellulose, nitroglycerine, cordite and dynamite were developed and considered as a rocket propellant. Immediately before World War I, the French used nitro-cellulose as a propellant for artillery rockets.

Before World War II were developed the first composite propellants using an organic matrix (asphalt) and an inorganic oxidizer (potassium perchlorate). After this development the specific impulse started to increase strongly.

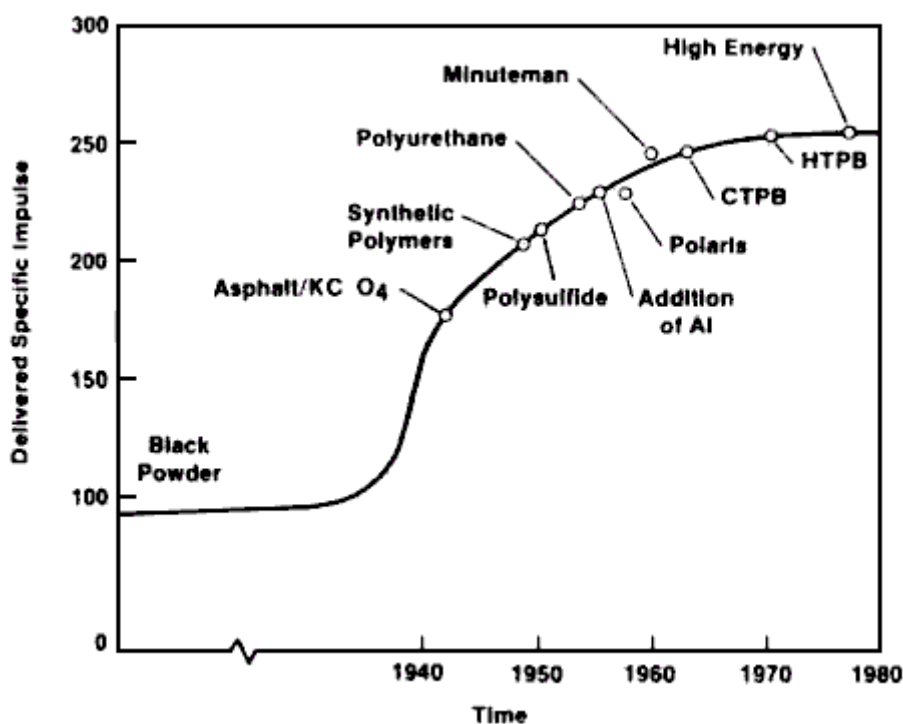


Figure 1 – Delivered Specific Impulse evolution³

In 1970's the specific impulse of the rockets stopped its continuous increase. It was due to all chemical reactions were discovered and there are no new chemical reactions to improve the specific impulse of the solid propellant rockets. Figure 1, from the **Encyclopedia Astronautica**, shows this trend

³ <http://www.astronautix.com/props/solid.htm#more>

where chemical reactions have a limit in terms of specific impulse. See <http://www.astronautix.com/props/solid.htm>

There are several solid propellant rockets used in space missions in the last years. Following, some examples are presented: Hercules, P230, Star37 and LGM-30.

1.1.1 Hercules – Space shuttle booster

Hercules was the solid rocket engine of the Space shuttle Columbia. It was the first space worthy space shuttle in NASA's orbital fleet. It completed 27 missions before disintegrating during re-entry on February 1, 2003. The destruction of the orbiter killed all the crew. It is known as SRB. See:

http://en.wikipedia.org/wiki/Space_Shuttle_Columbia
<http://www.astronautix.com/engines/hercules.htm>

1.1.2 P230 – Ariane 5 booster

P230 is the solid rocket engine of the Ariane 5. It is a part of Ariane rocket family and is an expendable launch system used to deliver payloads into Geostationary Transfer Orbit (GTO) or Low Earth Orbit (LEO). They are manufactured under the authority of the European Space Agency (ESA). See:

<http://www.astronautix.com/engines/p230.htm>

1.1.3 Star37 – FLTSTACOM satellite

Star37 engine⁴ was the apogee kick motor of the FLTSTACOM satellite. It was a 20th century satellite communication system for the U.S. Navy and was used for UHF communications between ships, submarines, airplanes and ground stations of it. See:

<http://www.astronautix.com/engines/star37fm.htm>

1.1.4 LGM-30 – Minuteman ICBM

LGM-30 was the solid rocket engine of the Minuteman ICBM. It is an U.S. nuclear missile, a land-based intercontinental ballistic missile (ICBM). It is one component of a nuclear triad. The letter "L" in "LGM" indicates that the missile is silo-launched, the "G" indicates that it is designed to attack ground targets and the "M" indicates that it is a guided missile. See:

http://es.wikipedia.org/wiki/LGM-30_Minuteman
<http://www.astronautix.com/stages/minn1at1.htm>

1.1.5 Summary of the technical parameters

In table 1 a summary of technical parameters for every solid propellant implementation is presented. Our WikiLauncher will require a smaller engines with high performances.

⁴ <http://www.ltas-vis.ulg.ac.be/cmsms/uploads/File/DataSheetSolidATK.pdf>

Table 1 – Solid propellant rocket technical parameters summary

	Hercules	P230	Star37	LGM-30	WikiLauncher
Gross mass (kg)	625,000	269,000	1,147	22,900	2.6
Unfuelled mass (kg)	75,000	34,000	81	2,500	1.17
Propellant mass fraction	88%	87%	93%	89%	55%
Height (m)	38.41	31	1.68	7.50	0.29
Diameter (m)	3.81	3	0.93	1.68	0.07
Thrust (kN)	15,566	6,472	47.9	792	1
Specific impulse (s)	286	286	290	288	201
Specific impulse sea level (s)	259	259	270	268	181
Burn time (s)	133	63	63	56	7

1.2 WikiLauncher

WikiLauncher is the name of the launcher that Wikisat team⁵ uses in order to put satellites in orbit. This launcher will inject into low orbit up to 6 femto-satellites. This process is carried out in two stages. First of all, the payload is raised with a latex balloon filled with helium. First stage achieves an apogee altitude of 250 km. In table, the first stage of the WikiLauncher is compared with other engines. This engine is at the state achieved at this work. Additional improvements should be achieved in order to be competitive. In the second stage, the rocket propels the satellites and puts them into orbit.

Other teams have designed the satellite, the balloon and the terrestrial stations. We will do a detailed design of the rocket. Other students have studied some rocket systems before, like the vector control or the preliminary nozzle design. Until now, calculus and designs have not been proved with so many real tests as the Wikisat team has done.

⁵ <http://www.wikisat.org>

CHAPTER 2. ENGINE STRUCTURE VALIDATION

In this chapter some components are selected to be used as a structure for the rocket. A Soda Can will be proposed as the main container thanks to its light weight and high volume, achieving a propellant mass fraction about 80%. This selection is suitable for the WikiLauncher second stage where high performance is required. First block studies the Soda Can (Steel Coke Can) behaviour in terms of weak structural points (Crack propagation, flanges, and bulkhead). Some pressure test will be done. Due to this structure will have a very high thermal load, the steel material study is required. In addition, the solid propellant (APCP or Candy) inside the rocket structure should be taken into account.

The hypothesis of using Commercial-Off-The-Shelf (COTS) as an engine container for our launch second stage is proposed. In our case a steel Soda Can will be used. The maximum reachable pressure and the approximate melting point will be tested in several Can models. The rest of the rocket design will be adequate to these limits. Other COTS will be considered like a Spray FOAM Can and an Argon Welding Bottle. These other selections are suitable for the WikiLauncher first stage.

2.1 Structure selection and mechanical study

First block studies the Soda Can behavior in terms of weak structural points (Crack propagation, flanges, and bulkhead). Some pressure test will be done.

A Soda Can is used instead of the usual steel cylinder because it is necessary to reach a less than 20% Dry to Wet Mass Ratio in structure. Otherwise, this rocket will not can be put into orbit. In amateur rocket making, steel pipes of less than 1 millimeter thick are used. This way guarantees the hardness of the structure at the expense of getting a 50% Dry to Wet Mass Ratio, which means that the structure weight equals to the propellant weight. Having a rocket of these properties it is possible to reach the space but an orbit velocity cannot be achieved.

Table 2 – Physical parameters and maximum pressure for each vessel

	Cesaroni O3700	AMW N2800	AeroTech N4800
Diameter (m)	0.161	0.098	0.098
Lenght (m)	0.957	1.213	1.201
Propellant weight (kg)	17.157	7.695	9.571
Total weight (kg)	31.351	13.809	14.784
Propellant mass fraction	54.7%	55.7%	64.7%
Average thrust (N)	3,654.3	2,764.1	4,800
Maximum thrust (N)	4,081.6	3,654.3	6,599.4
Total impulse (Ns)	29,919.9	14,801.7	19,361
Burn time (s)	8.2	5.4	4.4

As said before, there are several amateur rockets available in the market. Their thrusts are over 1 kilonewton but their propellant mass fractions are below 65%. Therefore, they cannot be put into orbit. Table 2 shows some technical parameters of three amateur rockets.

2.1.1 Soda Can manufacturing

The can material is extracted from a big coil of steel and tin. See a **Discovery Channel** documental⁶. On this big metallic sheet are stamped some flat disks. This procedure is carried out by a press with a speed of 2,500 disks per minute. After that, the structure owners give the characteristic cylindrical shape to the disks. In order to avoid the oxide that the liquid can produce, the interior of the can is sprayed with an epoxy resin. The next step is to paint the cans for its commercial use. To assure that the paint is adhered to the can surface they are transported to an oven cure. Then the upper part of the can is compressed to create the neck. It is compressed until achieve a diameter reduction of 10%. Later the cans arrive to an inspection area where a light detects possible holes in the structure. Quality controls are done each 15 minutes. It means that a can is selected every 30,000. Finally, the cans are filled with refreshment and they are sealed hermetically with a double junction.

The can has a curved bulkhead in case of the liquid freezes inside. In this case, the pressure would increase and the bulkhead would absorb the increasing volume. In our case, the pressure relief point will be the working parameter giving a margin before break.

In the market, a can is a cheap and easy to buy product. After a verification process, this Can is a suitable COTS for a rocket.

2.1.2 Soda Can integration

The neck of the can will be bended against the nozzle flange in order to close the assembly. This metallic closing ensures a hermetically union, it does not require a joint that could be burned and at the same time it is a reinforcement for the neck can. Inside the can, a layer of ablative material will protect the can structure from the high temperatures. Centered, there is a cylinder of propellant in such a way the flame progresses from the end (nozzle side) to the front. Due to there is no nozzle available in the domestic market that fulfils our needs it must be made on purpose. The fuel will define the design parameters which will be explained in chapter 3: the temperature, the burn time, etc. The selected structure will determine the operating pressure. Finally, we will design the nozzle to fulfill these parameters set by the propellant and the can structure.

2.1.3 Mechanical properties study

One of the most important constructive parameters of the engine is the maximum pressure that it can hold up. In this section, a theoretical study is done in order to calculate the pressure⁷ before breaking. It is calculated for three structures: a red Coke Can, a black Coke Can and an Argon bottle. These three containers are considered cylindrical vessels and they are made of steel.

⁶ <http://www.youtube.be/EzLhSzMCGDI>

⁷ http://en.wikipedia.org/wiki/Pressure_vessel

The maximum pressure formula (1.2) for a cylindrical vessel is:

$$P_{max} = \frac{M\tau}{2\pi R^2(R+W)\rho} \quad (1.2)$$

where **M** is the mass of the vessel, τ is the maximum work stress that the material can tolerate, **R** is the radius, **W** is the width and ρ is the density of the vessel material. In table 3 are shown the parameters⁸ of each vessel and the calculus of the maximum pressure.

Table 3 – Physical parameters and maximum pressure for each vessel

	Red Coke Can	Black Coke Can	Argon bottle
Density (Kg/m³)	7,840	7,840	7,840
Maximum work stress Ultimate Tensile Stress (MPa)	726	726	726
Mass (g)	25	22	1,120
Radius (mm)	30	22.5	32.5
Width (mm)	117	139	270
Maximum pressure (Bar)	27.85	30.31	517.46
Manufacturer maximum pressure (Bar)	18	20	165
Safety margin	1.55	1.52	3.14

In the case of the argon bottle, the manufacturer provides a value for the maximum pressure: 165 Bar. In this section it is shown that the theoretical maximum pressure is 517.46 Bar. Therefore, the manufacturer leaves a safety margin of 3.14 times.

In the following graph it is shown the relation between the structure maximum pressure and its mass for a given values of ultimate tensile stress, radius, width and density. Maximum pressure is proportional to mass as shown in the figure 2(a).

⁸ <http://www.matweb.com/>



Figure 2 – (a) Max pressure vs Mass and (b) Crack propagation

2.1.3.1 Pressure test 1

Red can model. In the first test, the bulkhead has budged. Immediately later, the can structure has escaped from the subsection.

2.1.3.2 Pressure test 2

Red can model. In this test, due to the can was not properly subjected, it has escaped before achieving the maximum reachable pressure. The bulkhead has budged before.

2.1.3.3 Pressure test 3

Red can model. In this test, the results are the same as the previous test. It also can be observed that the bulkhead budges at 8 bar pressure. The can escape from the subsection when it reaches 12 bar pressure.

2.1.3.4 Pressure test 4

Red can model. This test has been the first success. Due we added a wire in order to give some subsection to the can, the can has not escaped from the

subjection until it has been broken. The bulkhead budged at 8 bar pressure and the structure reaches its maximum pressure at 15 bar just before breaking.

2.1.3.5 Pressure test 5

Red can model. In this test, it has been tested to put the wire in the central part of the can instead of putting it on the neck like previously done. The bulkhead budged at 8 bar pressure. The can has escaped from the subjection at 16 bar pressure, without breaking. A deformation of the subjection part of the can is observed.

2.1.3.6 Pressure test 6

Red can model. In this test, the wire was located both in the neck part and the central part of the can. The bulkhead budged at 8 bar pressure. The can broke at 16 bar pressure.

2.1.3.7 Pressure test 7

Black can model. This test has been done with a different kind of can (longer and narrower). The wire was located at the neck. The bulkhead budged at 8 bar pressure and the can has escaped from the subjection at 14 bar pressure.

2.1.3.8 Pressure test 8

Black can model. In this test, the wire was located in the neck. The bulkhead budged at 8 bar pressure. The can broke at 16 bars. It can be observed that the structure broke on the top part of the can. There was no crack that propagated to the central part of the can.

2.1.3.9 Pressure test 9

Black can model. In this test we put an special reinforcement in the can neck. It consists of another neck of another can that was sealed. The bulkhead budged at 8 bar pressure. The can escaped from the subjection at 16 bar pressure while deforming the subjection part without producing any crack.

2.1.3.10 Pressure test 10

Black can model. In this test, the reinforcement was put as the previous test. The bulkhead budged at 8 bar pressure. The structure reaches its maximum pressure at 18 bar, and two cracks were propagated all the can long. Until now, this is the maximum pressure reached by a can.

2.1.3.11 Pressure test 11

This test was the first in which we used proper new equipment. It was achieved for the second time to blow up a black model can with the same reinforcement as tests 9 and 10. A precision pressure gage was used. The bulkhead budged at 10 bar pressure and the structure broke at 19 bar pressure, so 15 bar pressure can be the operating pressure. Figure 3 shows how the crack propagated along four branches. Typical failure point is in the upper flange as seen in the figure 2(b).

2.1.4 Summary of pressure tests

This section is a summary of pressure tests that were explained in section 2.1.3 and presented in Table 1. Test 11 shows a higher maximum pressure for bulkhead and burst due to a different pressure gage calibration.

Table 4 - Drag summary from previous sections

Pressure test	Can type	Maximum pressure (Bar)	
		Bulkhead	Can structure
Pressure test 1	Red can	Bulkhead	-
		Can structure	-
Pressure test 2	Red can	Bulkhead	Failed
		Can structure	Failed
Pressure test 3	Red can	Bulkhead	8
		Can structure	Failed at 12
Pressure test 4	Red can	Bulkhead	8
		Can structure	15
Pressure test 5	Red can	Bulkhead	8
		Can structure	Failed at 16
Pressure test 6	Red can	Bulkhead	8
		Can structure	16
Pressure test 7	Black can	Bulkhead	8
		Can structure	Failed at 14
Pressure test 8	Black can	Bulkhead	8
		Can structure	Failed at 16
Pressure test 9	Black can	Bulkhead	8
		Can structure	Failed at 16
Pressure test 10	Black can	Bulkhead	8
		Can structure	18
Pressure test 11	Black can	Bulkhead	10
		Can structure	19

2.2 Structure thermal load study

Due to this structure will have a very high thermal load, the steel material study is required. The thermal load study and the vibrations study are complicated to perform because it is easy to reach the maximum pressure. So we decided to begin the tests with another container with higher pressure tolerance: an Argon bottle that has a burst pressure of 165 Bar instead of 19 Bar for the Soda Can.

2.2.1 Combustion chamber pressure simulation

In figure 3(a), it can be seen how the bottle is deformed by the internal pressure and the force on the exit of the nozzle, caused by the exhaust of the fluid. Figure 3(b) shows the original shape of the bottle and the nozzle, which makes easier to appreciate the relative deformation. Finally, figure 3(c) shows a real case of how the bottle is deformed. See a YouTube video of the Stage1 Burn 06th:

<http://www.youtube.com/watch?v=xIRSAT0ghlo> burn 06th

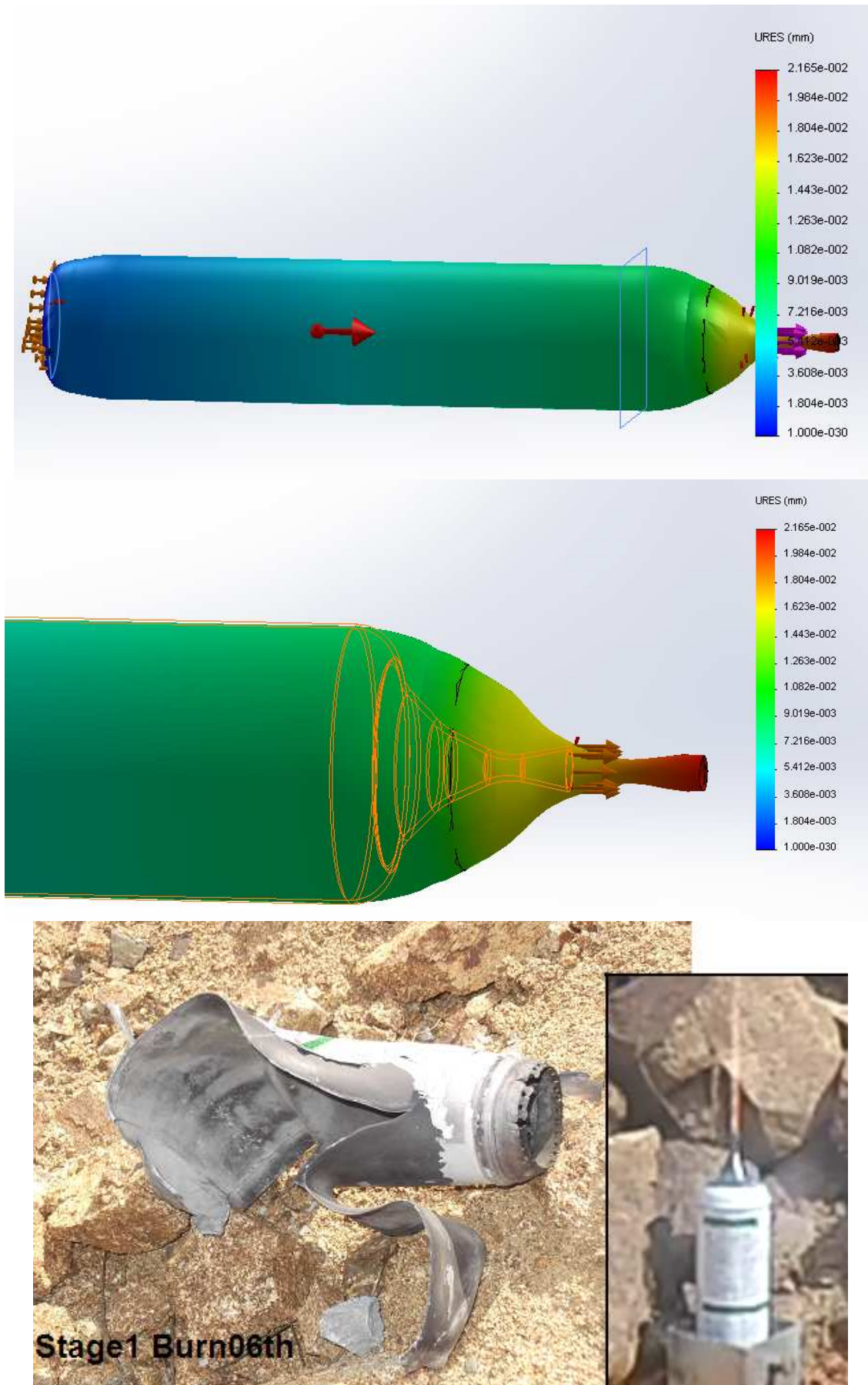


Figure 3 – (a) Deformations, (b) Relative to the original shape and (c) Real case

2.2.2 Combustion chamber pressure estimation

In this section, some pressure estimations of the combustion chamber were done by simulations. See 3.4 performance calculations section. The aim was to obtain the working pressure and four thermal tests were carried out. In the following sections the results are presented.

2.2.2.1 Thermal test 1

In this first thermal test a soda can was filled with solid propellant and it was connected to a pressure gage at the bottom of the can. Its range was 300 bar. The combustion started but the pressure gage showed null pressure. This pressure value remained until the end of the test. It was thought that the pressure gage range was too high.

See Burn38th http://www.youtube.com/watch?v=Gr0stq8_djs

2.2.2.2 Thermal test 2

In this second thermal test the same procedure was done. However, another pressure gage was used. Its range was 60 bar but the results were identical. The pressure gage showed a 0 bar pressure since the beginning until the end of the test. It was due to the nozzle does not retain air because it was not well designed.

See Burn39th <http://www.youtube.com/watch?v=P6t5VLxi8cc>

2.2.2.3 Thermal test 3

In this third test, as in the previous tests, the pressure sensor was put in the nozzle side in order to check the working pressure. After that, the can was filled with solid propellant as in the previous tests. This time, the ignition failed and it was not possible to calculate any value of pressure.

See Test <http://www.youtube.com/watch?v=4A-BQ4mSETk>

2.2.2.4 Thermal test 4

In this fourth test, an argon bottle was used. It was filled with propellant and had a nozzle designed on purpose for the second stage. This structure was thought for the first stage and it has a worse propellant mass fraction (55%). The ignition started but the structure exploded immediately due to an excess of powder. Later tests showed that the explosion was due to a lack of ablative material. Before exploding it was seen a proper flame but it last less than 1 second.

See test <http://www.youtube.com/watch?v=sPDQE7tLEQ0>

2.2.2.5 Thermal test 5

In this fifth thermal test, the same procedure was carried out. The argon bottle was filled with APCP and the nozzle was attached with screws to the structure. The ignition started but the structure exploded again. However, there was a proper flame before the explosion. This time, it was due to a lack of ablative material between the structure metal and the cylinder of propellant. The flame entered between them creating an important pressure increase until the bottle exploded.

See test <http://www.youtube.com/watch?v=xIRSAT0ghlo>

2.2.2.6 Thermal test 6

In the sixth thermal test, we tried to test the 4 mm throat nozzle to the limit but pressure increased suddenly and exploded in 10 seconds. During the Stage 1 burn 8th, the nozzle do not reached the red hot before the explosion. We can not assess the thermal capacity of this nozzle design for the moment.

2.3 Propellant study and selection

The solid propellant inside the rocket structure should be taken into account. It is important to select a propellant that fulfils the application parameters. This selection will determine some of them like burn rate and specific impulse. Therefore, it is need to study all the possibilities and select the one that best fits the requirements.

There are several families of solid propellants: Black powder, zinc-sulphur, candy, double-based and composite. In the following sections their advantages and disadvantages will be explained.

2.3.1 Black powder propellants

This family of propellants is used in pyrotechnic but also in amateur rocket models. Charcoal is used as fuel and potassium nitrate as the oxidizer. Sulfur is added as an additive. The specific impulse of this family of propellants is low (80 s) and their burn rate is fast.

2.3.2 Zinc-sulfur propellants

This family of propellants is used in amateur rocketry. Zinc is used as fuel and sulfur as the oxidizer. Its performance is poor due to its fast burn rate and low specific impulse (45 s).

2.3.3 Candy propellants

These propellants are also used in amateur rocketry. They are composed of an oxidizer and a sugar fuel. They have a fast burn rate and a low-medium specific impulse (130 s) and that is the reason why they are proper for amateur rocketry but not for advanced rockets.

2.3.4 Double-based propellants

This family of propellants is used in applications where medium-high specific impulse is required as medium-advanced rocketry. They are composed of two monopropellants. One of them can achieve the specific impulse required because has more energy than the other. The function of the second one is to control the instability that the first one can provide. Its specific impulse is 235 s and they have a medium burn rate.

2.3.5 Composite propellants

These propellants are used in professional rocketry due to their high specific impulse (between 210-265 s) and their low burn rate. They are composed for a powdered oxidizer like ammonium perchlorate (AP) and ammonium nitrate (AN) and aluminum or magnesium as fuel. Propellants based on AN have less specific impulse than propellants based on AP but they are more toxic. A binder holds these components as a grain.

2.3.6 Propellant selection

Once all the propellants have been studied it is needed to choose one that best fits the necessities of our application. Black powder propellants are very fast and easy to obtain but the Isp are too low. Furthermore, they are very dangerous because they can ignite easily. Zinc-sulfure propellants are very contaminants and their Isp are poor too. Candy propellants are easy to obtain like black powder ones. They burn quickly and their Isp are medium high but they can burn easily during the elaboration process so they are discarded too. Double-based propellants have a high Isp but they are used in military field and therefore hard to obtain. Finally, materials used for composite propellants are easy to buy and the specific impulse of them is one of the bests. They do not burn easily because it is needed a very high flame temperature during a long time. Therefore, **composite propellants are selected**.

We call C1 to the combination of a mixture between Ammonium Perchlorate and Styrene in a ratio of 70/30 in mass. We call C2 to the combination of a mixture between Ammonium Perchlorate, Styrene and Aluminium powder in a ratio of 70/23/7 in mass. C2 propellant has a higher specific impulse than C1 propellant but C2 propellant has a higher burn temperature.

Related to composite propellants, Wikisat team experience has proved that it is very difficult to ignite during the mixture. It can only burn if the propellant is near an intense flame about 320 °C. Logically, it must not happen at room temperature. Several safety measures are taken when this process is carried out as detailed in chapter 5 in the environmental impact study.

CHAPTER 3. NOZZLE DESIGN AND VALIDATION

In this section a nozzle based on previous requirements is designed and validated. The nozzle has to be adapted to the work needs and the propellant and the container design restrictions. Now it is not possible to use COTS so we make our own nozzle. Several simulations will be done. We based this study in a Computed Fluid Dynamics (CFD) module in **SolidWorks**.

3.1 Design parameters

This section is a selection of parameters related to the burn and its implications in the rocket performances. The study is based on a Richard Nakka's work⁹ about experimental burns of amateur propellant like Candy, Dextrose and Sorbitol.

3.1.1 Burn rate

Propellant burning rate is influenced by certain factors, the most significant being:

- Combustion chamber pressure
- Initial temperature of the propellant grain
- Velocity of the combustion gases flowing parallel to the burning surface
- Local static pressure
- Motor acceleration and spin

The usual representation of the pressure P_c dependence on burn rate is the Saint Robert's Law (3.1) also known as Vieille's Law:

$$r = r_0 + aP_c^n \quad (3.1)$$

where r is the burn rate, r_0 is a constant (usually taken as zero), a is the burn rate coefficient, and n is the pressure exponent. The values of a and n are determined empirically for a particular propellant formulation, and cannot be theoretically predicted. It is important to realize that a single set of a , n values are typically valid over a distinct pressure range. More than one set may be necessary to accurately represent the full pressure regime of interest

Temperature affects the rate of chemical reactions and thus the initial temperature of the propellant grain influences burning rate. If a particular propellant shows significant sensitivity to initial grain temperature, operation at temperature extremes will affect the time-thrust profile of the motor. This is a factor to consider for winter launches, for example, when the grain temperature may be 20 °C or more lower than "normal" launch conditions.

For most propellants, certain levels of local combustion gas velocity (or mass flux) flowing parallel to the burning surface leads to an increased burning rate. This "augmentation" of burn rate is referred to as erosive burning, with the extent varying with propellant type and chamber pressure. The mechanism of increased convective heat transfer to the propellant surface due to turbulence is

⁹ <http://www.nakka-rocketry.net/burnrate.html>

most likely responsible for this augmentation. For many propellants, a threshold flow velocity exists. Below this flow level, either no augmentation occurs, or a decrease in burn rate is experienced (negative erosive burning).

In an operating rocket motor, there is a pressure drop along the axis of the combustion chamber, a drop which is physically necessary to accelerate the increasing mass flow of combustion products toward the nozzle. The static pressure is greatest where gas flow is zero, that is, at the front (bulkhead) of the motor. Since burn rate is dependent upon the local pressure, the rate should be greatest at this location. However, this effect is relatively minor and is usually offset by the counter effect of erosive burning.

Burning rate is enhanced by acceleration of the motor. Whether the acceleration is a result of longitudinal force (e.g. thrust) or spin, burning surfaces that form an angle of about 60° to 90° with the acceleration vector are prone to increased burn rate. As the majority of the burning surface of most grain configurations is perpendicular to the motor axis, spin (rather than longitudinal acceleration) has a far more profound effect on burning rate. There are three main reasons why spin increases burn rate:

- Rotation reduces the mass flux (flow) at the nozzle throat. This reduction in mass flux has the same effect as a decrease in throat area, thus increased chamber pressure (and consequently higher burning rate) may result.
- Viscous flow patterns are set up in the motor, increasing heat transfer to the propellant surface through greater mass transfer.
- The radial acceleration forces can cause greater retention of the solid phase combustion products near the propellant surface.

3.1.2 Mass flow

Mass generation rate of combustion products is defined by (3.2):

$$M_{gen} = \frac{(m_0 - m_1)}{(t_1 - t_0)} \quad (3.2)$$

Mass flow rate through nozzle can be calculated using (3.3):

$$M_{gen} = \frac{(P_0 - P_{atm})A}{\sqrt{Rt_0}} \sqrt{k} \left(\frac{2}{k+1} \right)^{\frac{(k+1)}{k-1}} \quad (3.3)$$

Where:

k is the ratio of specific heats.

R is the specific gas constant.

t₀ is the chamber temperature

Obviously, mass storage rate of combustion products can be calculated with $M_{gen} - M_{noz}$.

Empirically we know that mass flow is 0.7 g/s at atmospheric pressure, without nozzle and for a burning section of 66 mm diameter.

3.1.3 Throat diameter

The throat diameter must be large enough to ensure that the combustion chamber maximum pressure, which is determined by the material that is used in the structure, is not achieved.

The k_n (Ratio of burning area to throat area) is a key design parameter that sizes the throat diameter and determines chamber pressure.

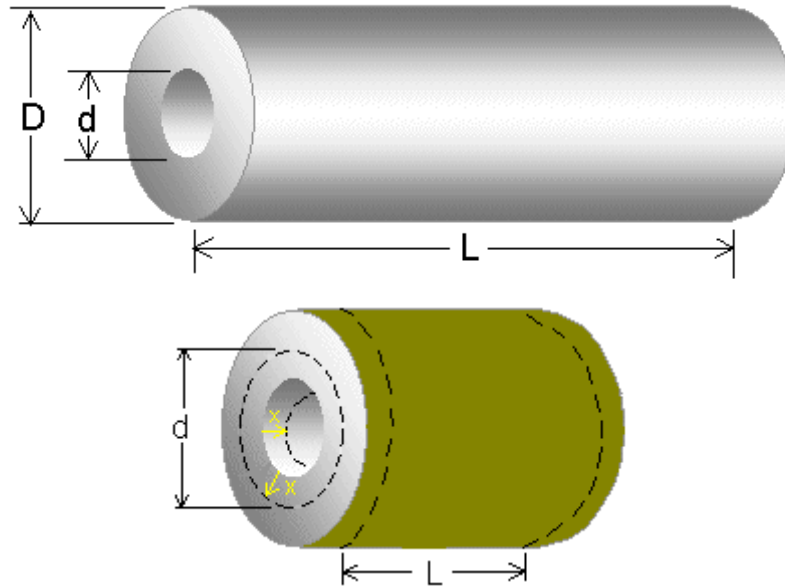


Figure 4 – Propellant grain dimensions

As Nakka presented¹⁰, the burning surface area for a hollow-cylindrical grain, as shown in Figure 4, may be calculated in one of these three burn types:

- Grain with unrestricted burning (no surfaces inhibited):
- Grain with outer surface inhibited (burning at core and ends):
- Grain with both ends inhibited (burning on outer surface and core):

Grain with unrestricted burning:

$$A_{b \max} = A_{b \text{ initial}} = \frac{1}{2} \pi(D^2 - d^2) + \pi L(D + d)$$

$$A_{b \text{ final}} = \pi(D + d)(L - t)$$

$$\text{where } t = \frac{1}{2}(D - d) \quad (3.4)$$

Grain with outer surface inhibited:

$$A_{b \max} = A_{b \text{ initial}} = \frac{1}{2} \pi(D^2 - d^2) + \pi dL$$

$$A_{b \text{ final}} = \pi D(L - 2t) \quad (3.5)$$

Grain with both ends inhibited:

$$A_b = \text{constant} = \pi L(D + d) \quad (3.6)$$

The instantaneous grain burning surface area is given by equation (3.7):

¹⁰ <http://www.nakka-rocketry.net/design1.html>

$$A_b = N \left[\frac{1}{2} \pi (D^2 - d^2) + \pi L d \right] \quad (3.7)$$

where \mathbf{N} is the number of segments; \mathbf{d} and \mathbf{L} are the instantaneous values of core diameter and segment length (See figure 4), and are given by equation (3.8):

$$\begin{aligned} d &= d_0 + 2x \\ L &= L_0 - 2x \end{aligned} \quad (3.8)$$

where \mathbf{x} is the linear surface regression (distance the web has burned, normal to the web surface).

The initial and final burning surface areas are given by equation (3.9):

$$\begin{aligned} A_{b \text{ initial}} &= N \left[\frac{1}{2} \pi (D^2 - d_0^2) + \pi L_0 d_0 \right] \\ A_{b \text{ final}} &= N \pi D (L_0 - 2t) \\ t &= \frac{1}{2} (D - d_0) \end{aligned} \quad (3.9)$$

The value of \mathbf{x} when the burning surface area reaches maximum is important as this determines maximum chamber pressure. This value of \mathbf{x} may be found by setting the derivative (represented by the slope of the \mathbf{k}_n vs web regression curve) to zero (i.e. $dA_b/dx = 0$), then solving for \mathbf{x} .

As such, the value of \mathbf{x} is found to be in equation (3.10):

$$x = \frac{1}{6} (L_0 - 2d_0) \quad (3.10)$$

at $\mathbf{A}_{b \text{ max}}$.

The value of $\mathbf{A}_{b \text{ max}}$ is then found by substituting \mathbf{x} into Eqns. 3.6 to find \mathbf{d} and \mathbf{L} , then substituting these values into equation (3.5).

Note that the \mathbf{k}_n profile is progressive if the calculation gives $\mathbf{x} > d_0$. In this case, $\mathbf{A}_{b \text{ max}} = \mathbf{A}_{b \text{ final}}$. The \mathbf{k}_n profile is regressive if the calculation gives $\mathbf{x} < 0$. In this case, $\mathbf{A}_{b \text{ max}} = \mathbf{A}_{b \text{ initial}}$.

When designing a rocket motor, the dimension \mathbf{D} is usually limited by factors such as casing or fuselage size. The choice of core diameter, d_0 , is usually based upon desired web thickness (which determines burn time) and erosive burning considerations. Thus, segment length, \mathbf{L}_0 , is the parameter that may be available to control the \mathbf{k}_n profile. The value of \mathbf{L}_0 may be found which gives a symmetric \mathbf{k}_n profile (initial and final \mathbf{k}_n are equal), if \mathbf{D} and \mathbf{d}_0 are specified:

$$L_0 = \frac{1}{2} (3D + d_0) \quad (3.11)$$

for symmetric profile

3.1.4 Velocity of the exhaust

The velocity of the exhaust is intended to be as high as possible. Due to the rocket obtains its thrust by turning caloric energy to kinetic energy we can represent it by the following equation (3.12):

$$h_1 - h_2 = \frac{1}{2}(v_2^2 - v_1^2) = C_p(T_1 - T_2) \quad (3.12)$$

where a particle of fluid goes from point 1 to point 2 and:

h is the fluid enthalpy

v is the fluid velocity

C_p is the fluid caloric capacity

T is the fluid temperature

The gas exhaust velocity (Mach number) is defined by the relation between the nozzle exit diameter and the throat diameter that was previously fixed.

We can also determine the velocity of the fluid in any point of the nozzle by using the following equation (3.13):

$$\frac{A}{A^*} = \frac{1}{M} \left(\frac{1 + \frac{k-1}{2} M^2}{1 + \frac{k-1}{2}} \right)^{\frac{k+1}{2(k-1)}} \quad (3.13)$$

Where **A** is the area of the nozzle at any point of the nozzle and **M** is mach number. The "*" refers to M=1 condition, when the fluid has sound velocity, this happens on the throat. That means that the exit velocity is determined by the relation between the exit area and the throat area.

$$V_e = \sqrt{2T_0 \left(\frac{R'}{M} \right) \left(\frac{k}{k-1} \right) \left[1 - \left(\frac{P_e}{P_0} \right)^{\frac{k-1}{k}} \right]} \quad (3.14)$$

Equation (3.14) is specifically useful to determine the velocity at the nozzle exit. It relates the exit velocity with the following parameters:

k: ratio of specific heats, obtained by the analysis.

R': gas constant (R=8.3143 N·m/mol·K).

M: effective molecular weight, obtained by a combustion analysis.

T₀: propellant combustion temperature, obtained by a combustion analysis.

P_e: exit pressure. It can be assumed equal to atmospheric pressure.

P₀: combustion chamber pressure.

The exhaust gases velocity is maximized changing the exhaust diameter for a given throat diameter.

3.1.5 Nozzle efficiency

The nozzle inner geometry defines the efficiency. Is the ratio between the actual thrust to the theoretical thrust. Typically 0.75 to 0.85 for dextrose, sorbitol or sucrose based propellants for a well-counteracted, smooth nozzle.

3.1.6 Burning time

The burning time depends on the amount of fuel that the structure (Bottle) is able to contain but mainly it depends on the burn type. End burner is slower than Core burner. The faster the burn, the better apogee is in the trajectory. In section 3.2.2 Construction parameters can be seen that from case 2 to case 6, the apogee altitude is every time greater. For each improvement in the grain, the burn time is every time smaller and then apogee is higher. We are interested in a fast burn time.

3.1.7 Thrust

Based on Tsiolkovski¹¹ equation (3.15), the theoretical thrust of a rocket is given by the following equation:

$$T = M_{flow}V_e + (P_e - P_0)A_e \quad (3.15)$$

M_{flow} : mass flow

V_e : Exit velocity

P_e : Exit pressure

P_0 : Atmospheric pressure

A_e : Exit area

The amount of thrust T produced by the rocket depends on the mass flow rate through the engine, the exit velocity of the exhaust, and the pressure at the nozzle exit. All of these variables depend on the design of the nozzle. The smallest cross-sectional area of the nozzle is called the throat of the nozzle. The hot exhaust flow is choked at the throat, which means that the Mach number is equal to 1.0 in the throat and the mass flow rate \dot{m} is determined by the throat area. The area ratio from the throat to the exit A_e sets the exit velocity V_e and the exit pressure P_e .

The generated thrust F is calculated in equation (3.16) is:

$$F = C_f N_{eff} P_0 A \quad (3.16)$$

Where:

F is the generated thrust.

C_f is a parameter called thrust coefficient.

N_{eff} is the nozzle efficiency.

P_0 is the absolute pressure.

A is the nozzle critical passage area which is the same as throat area

Thrust coefficient C_f is given by the equation (3.17):

$$C_f = \frac{P_e - P_{atm} A_{exit}}{P_0 A_t} + \sqrt{\frac{2k^2}{k-1} \left(\frac{2}{k+1}\right)^{\frac{k+1}{k-1}} \left(1 - \left(\frac{P_e}{P_0}\right)^{\frac{k-1}{k}}\right)} \quad (3.17)$$

Where:

k is the ratio of specific heats (the ratio of the heat capacity at constant pressure to heat capacity at constant volume)

P_e is the nozzle exit pressure

¹¹ <http://www.grc.nasa.gov/WWW/k-12/airplane/rockth.html>

P_{atm} is the atmospheric pressure

A_{exit} is the nozzle exit cross-section area

A_t is the throat cross section area

3.1.8 DeltaV

DeltaV is defined by the relation between the rocket total mass and the empty rocket mass. (Tsiolkovski equation) and the gas exhaust velocity which was previously given. This is a theoretical calculation where this change in velocity is instantly. In section 3.4 this time is taken into account when performance calculations are made. The faster the burn, the highest the deltaV is.

3.2 Nozzle design

This section contains the selected parameters for the final nozzle design.

3.2.1 Main parameters

These are the main nozzle parameters shown in figure 5

- Throat diameter: 4 mm
- Exit diameter: 10 mm
- Exit angle: 12°
- Bottle diameter: 70.6 mm
- Nozzle Expansion Ratio (A_e/A^*): 6.25

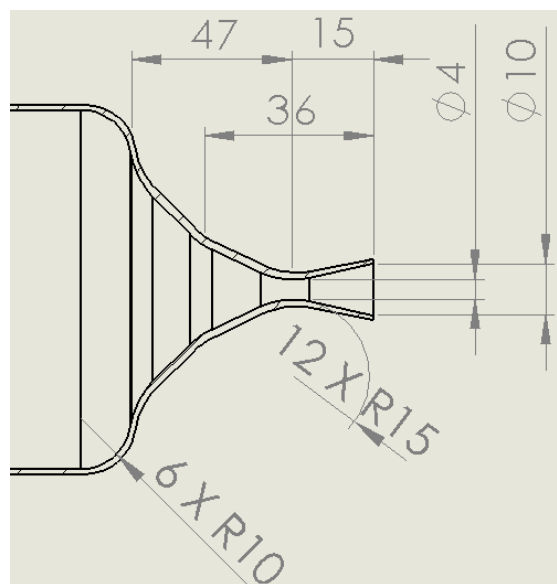


Figure 5 – Draft of main nozzle parameters

In order to increase the efficiency, the nozzle we designed has two different angles between the throat and the combustion chamber of 45° and 25° at 36 mm from the nozzle end. Obviously, not rounded parts are avoided.

3.2.1 Drawings

This section shows the manufacturer drawings for the nozzle and the combustion chamber as well as 3D models through figures 6 to 10.

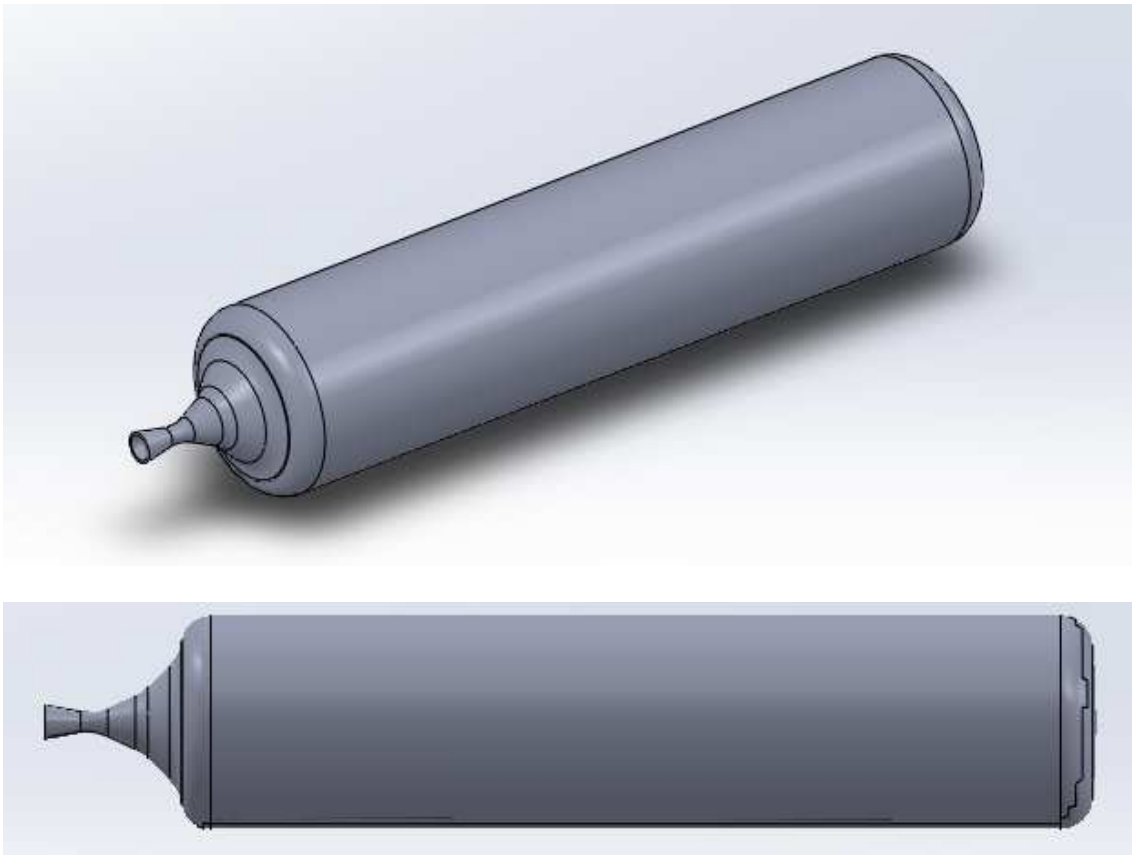


Figure 6 – 3D model for the bottle and the nozzle

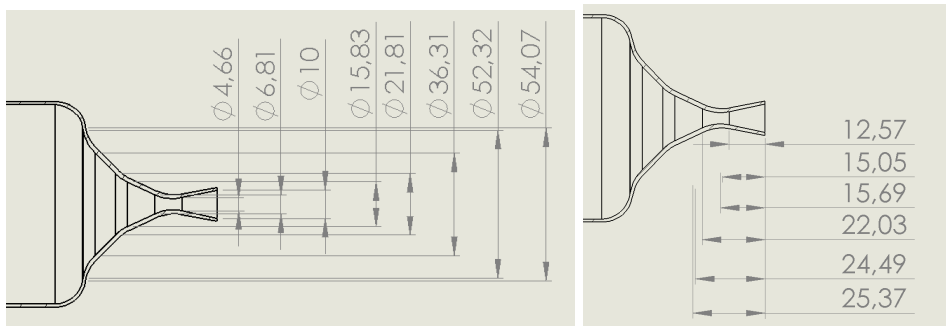


Figure 7 – Detailed nozzle parameters (I)

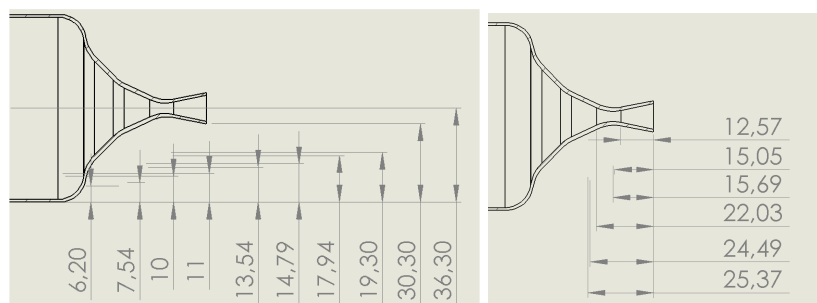


Figure 8 – Detailed nozzle parameters (II)

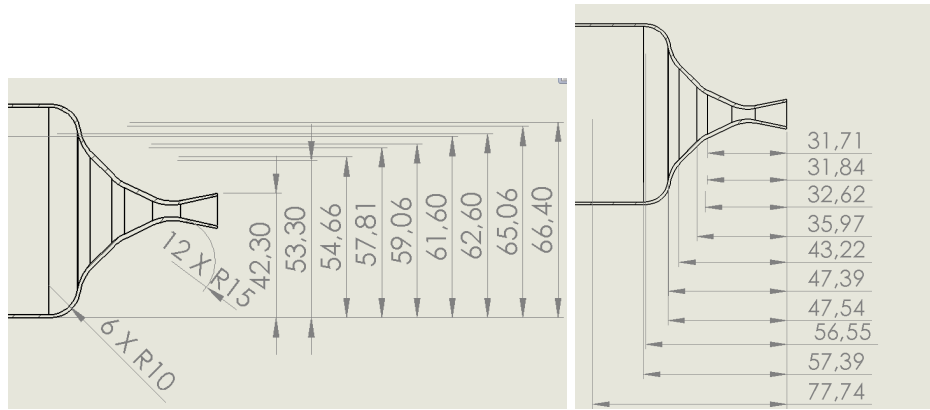


Figure 9 – Detailed nozzle parameters (III)

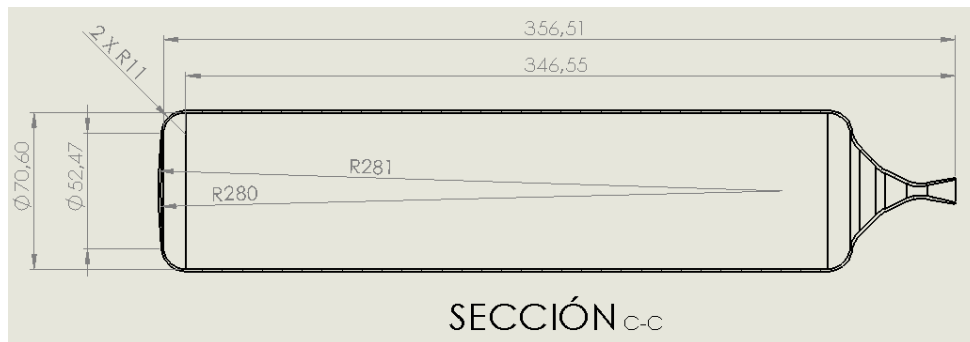
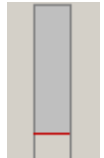
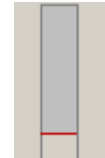
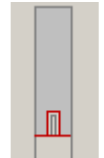
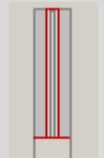
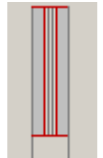
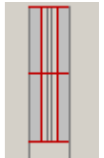


Figure 10 – Detailed bottle parameters

3.2.2 Construction parameters

We have performed series of simulations changing the throat diameter, the exhaust diameter and the type of burner in such a way we can compare different cases. Table 5 is a summary for these construction parameters for each serie that is detailed in the annex.

Table 5 - Summary for various cases of simulation series

Parameter	Case1	Case2	Case3	Case4	Case5	Case6
Throat diameter	2.4 mm	4 mm	4 mm	9 mm	9 mm	9 mm
Exhaust diameter	9.1 mm	10 mm	10 mm	26 mm	26 mm	26 mm
Expansion ratio	14.4:1	6.3:1	6.3:1	8.3:1	8.3:1	8.3:1
Total impulse	3.08 kN·s	2.63 kN·s	2.72 kN·s	2.76 kN·s	2.78 kN·s	2.79 kN·s
Specific impulse	222.7 s	190.6 s	197.0 s	201.3 s	202.6 s	203.6 s
Maximum thrust	101.45 N	45.28 N	294.72 N	976.79 N	726.43 N	533.35 N
Maximum pressure	152.6 atm	29.5 atm	163.6 atm	107.8 atm	81.8 atm	61.8 atm
Burnout time	30.22 s	58.13 s	46.76 s	7.03 s	6.70 s	6.44 s
Geometry type	End burner  Nozzle side	End burner  Nozzle side	Core burner Core length 33 mm Core diam. 6 mm  Nozzle side	Core burner Core length 220 mm Core diam. 6 mm  Nozzle side	Core burner Core length 225 mm Core diam. 6 mm  Both sides	Core burner Core length 112 mm Core diam. 6 mm  2 segments
Trajectory apogee	159.1 km	98.2 km	122.0 km	143.7 km	146.6 km	149.4 km

3.3 Burn type study and selection

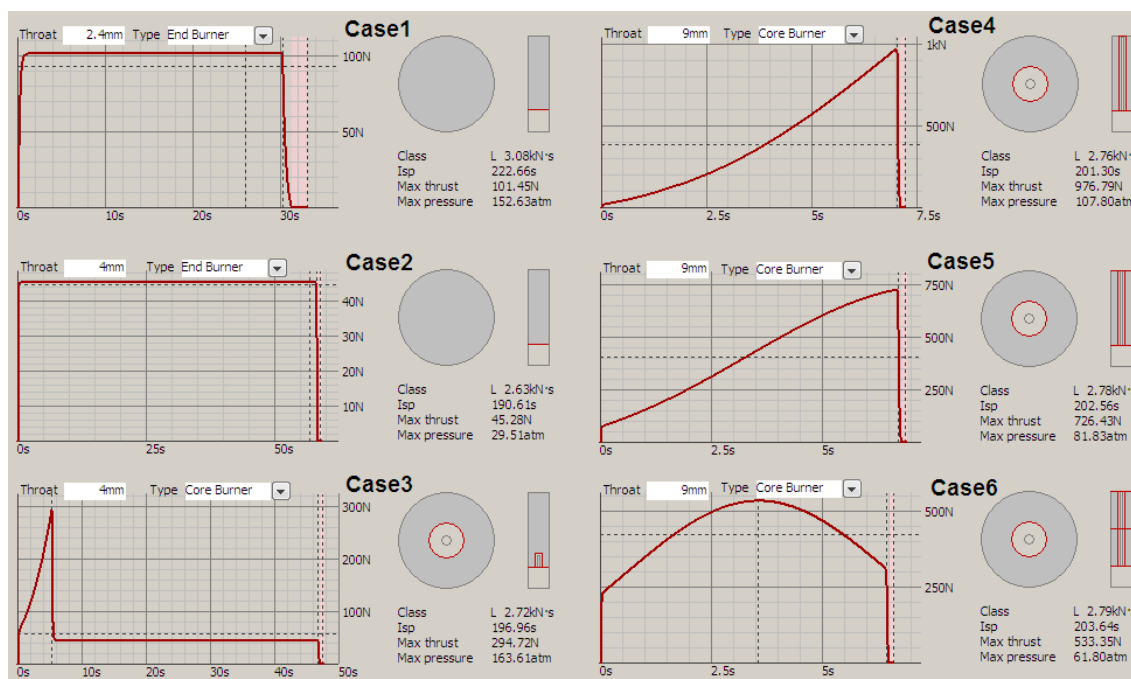


Figure 11 – Thrust vs time for each case

In this section, six burn cases are studied (See figure 11) in order to select the optimum burn configuration for the best trajectory in terms of maximum apogee.

The WikiSat team has got two types of nozzles, one with 4 mm throat and one with 9 mm throat. This is why simulations are using these sizes but we calculated the one with maximum specific impulse which corresponds to a 2.4 mm throat. The Case 1 optimizes the bottle parameters in terms of maximum pressure and total impulse, etc. but we do not have such a nozzle and burnout time is larger than other cases. In addition, this tiny nozzle should be made in tungsten instead of steel.

We look for the highest specific impulse possible. In table 5, the highest Isp is achieved by a small nozzle of 2.4 mm in diameter with the maximum thrust. The point is that, the faster burn, the better trajectory performance is because the gravity field is subtracting energy every second. The better case is the Case 6 but it is complicated to manufacture. Annex have the curve thrust vs time for each case were can be seen that Case 4 has a huge pressure peak while Case 5 and Case 6 are softer.

Figure 11 is a summary of each case in the same environmental conditions like, burned at same altitude, same C2 propellant, 1234 grams of dry mass, same throat efficiency of 85%, same payload (200 grams which corresponds to an IRIDIUM locator¹²), as can be seen in the annexes. Hence, the optimum case is the Case 4. Only an extra operation is required: to drill the core with a 6 mm bit in order to burn in only 7 seconds the 1.4 kg of propellant achieving an specific impulse of $I_{sp} = 201$ seconds and a maximum thrust of 977 N. As can be seen in table 5, the shorter burnout time, the greater trajectory apogee is, despite a lower specific impulse. This effect is due to the gravity force is relevant for every second of flight, more than specific impulse is.

3.4 Performance calculation

This section presents the final design performance calculations in terms of thrust vs time, pressure vs time and burn rate vs time for the burn case selected. For this purpose, we have designed a burner module in the open source **Moon2.0** simulator.

As presented in section 3.2.2 Construction parameters, the selected configuration was the case 4. Figure 12 has the curve of thrust vs time where thrust is increasing exponentially due to the burn cylinder is larger every time up to a limit. Figure 13 has the curve of pressure vs time where pressure is increasing exponentially as well. Figure 14 has the curve of burn rate vs time that is a lineal increase. These curves were generated by the simulator **Moon2.0** that uses the equations described in section 3.1 and **Nakka** simulator. The parameters selected are detailed in the annexes as well.

¹² <http://www.iridium.com/products/NAL-SHOUT-nano-Personnel-Tracker.aspx?productCategoryID=11>

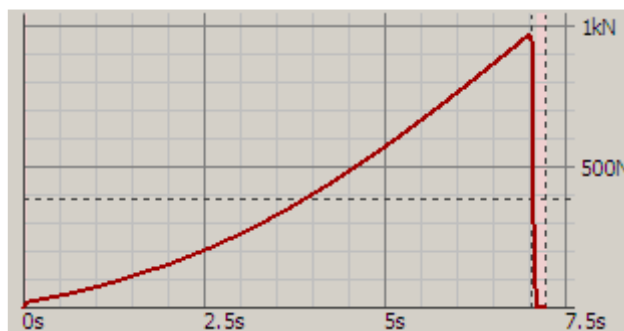


Figure 12 – Thrust vs time for the optimum case



Figure 13 – Pressure vs time for the optimum case

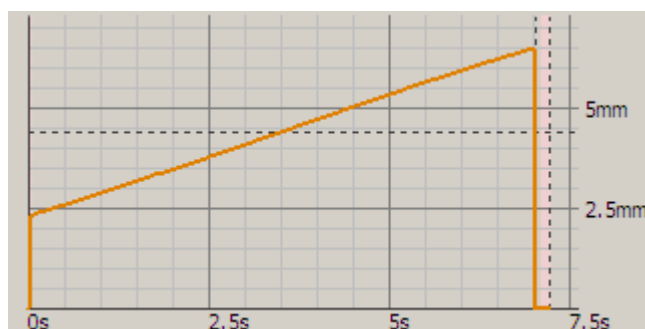


Figure 14 – Burn rate vs time for the optimum case

3.5 Nozzle validation

In this section we try to validate the nozzle under hard conditions of over-pressure, extended work time and thermal load. The nozzle was designed for the second stage but we have adapted the nozzle to the first stage to see the results. Obviously, the proper nozzle for the bottle is the 9 mm throat, not the 4 mm throat we show in figure 15. The picture corresponds to the Stage1 Burn06th where the nozzle worked for a moment before the explosion of the bottle in the quarry. The problem was due to the lack of ablative material between the metal and the propellant that worked as a large combustion section without an exit. The pressure increased in the combustion chamber ejecting the nozzle and at the same time, the bottle inflates until the burst happened. The flame size is similar to the simulation shown in the CFD picture.

We do not have measurement equipments in the real rocket so there is no way to compare the CFD results apart from visually means. Chapter 4 validates the burn simulation respect to the real burn comparing the burnout time which is a parameter that we can measure easily.

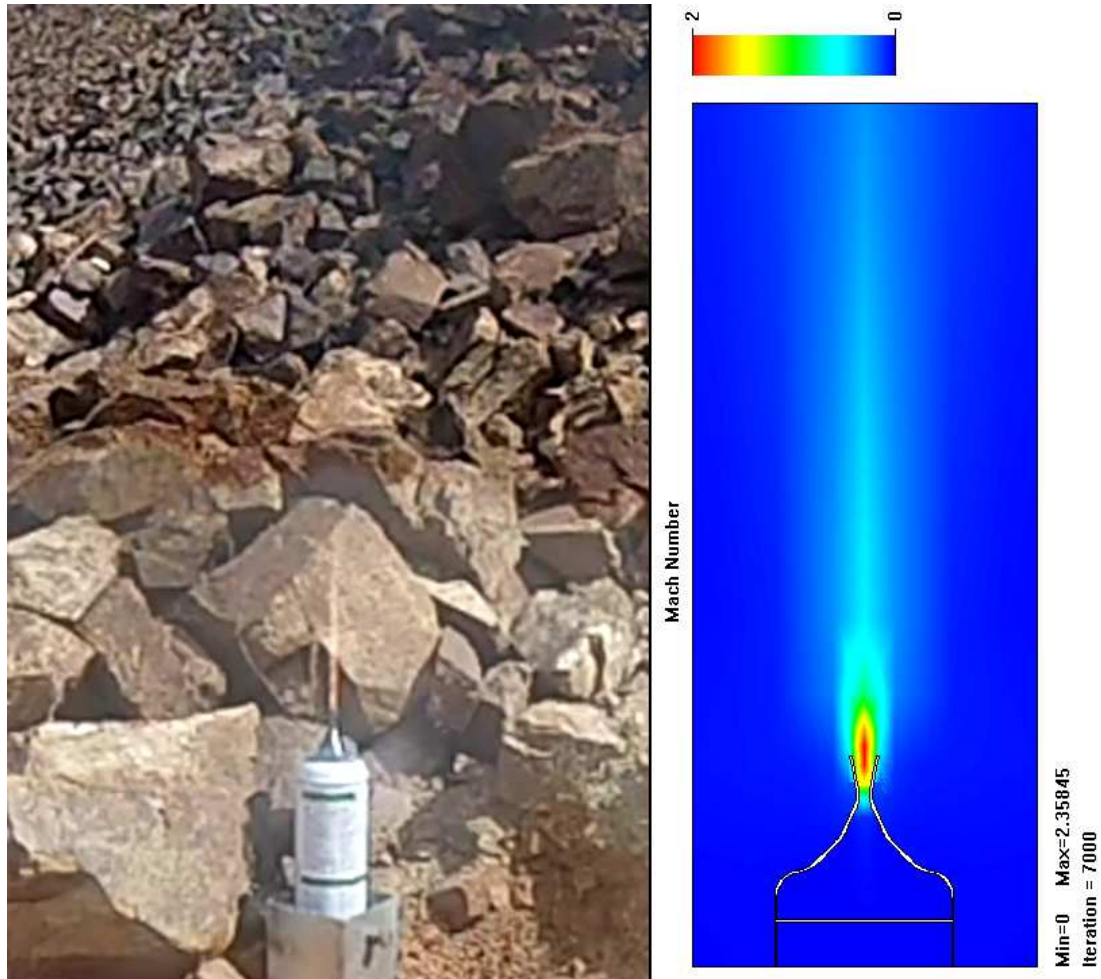


Figure 15 – Comparing real flame vs simulated flame

The figure 16 contains three Computed Fluid Dynamic simulations for total pressure in Pascals units, temperature in Kelvin units and total velocity in Mach number units. These simulations are time dependant and each one has a different moment. Pressure CFD shows how the internal nozzle shape is not relecant. Only pressure increase nearby the throat. The outside pressure is lower than the combustion chamber pressure as expected but lower than the Sea Level pressure, about 0.7 atmospheres. Temperature reaches to a stable value about 520 K. Finally, the Mach number CFD gives an idea of how the flow is accelerated in the subsonic/convergent nozzle side, the sonic flow located exactly in the throat and also accelerated in the supersonic/divergent nozzle side, reaching at 1.92 Mach after 1.27 ms. Details about CFD configuration and mesh data could be found in the annex.

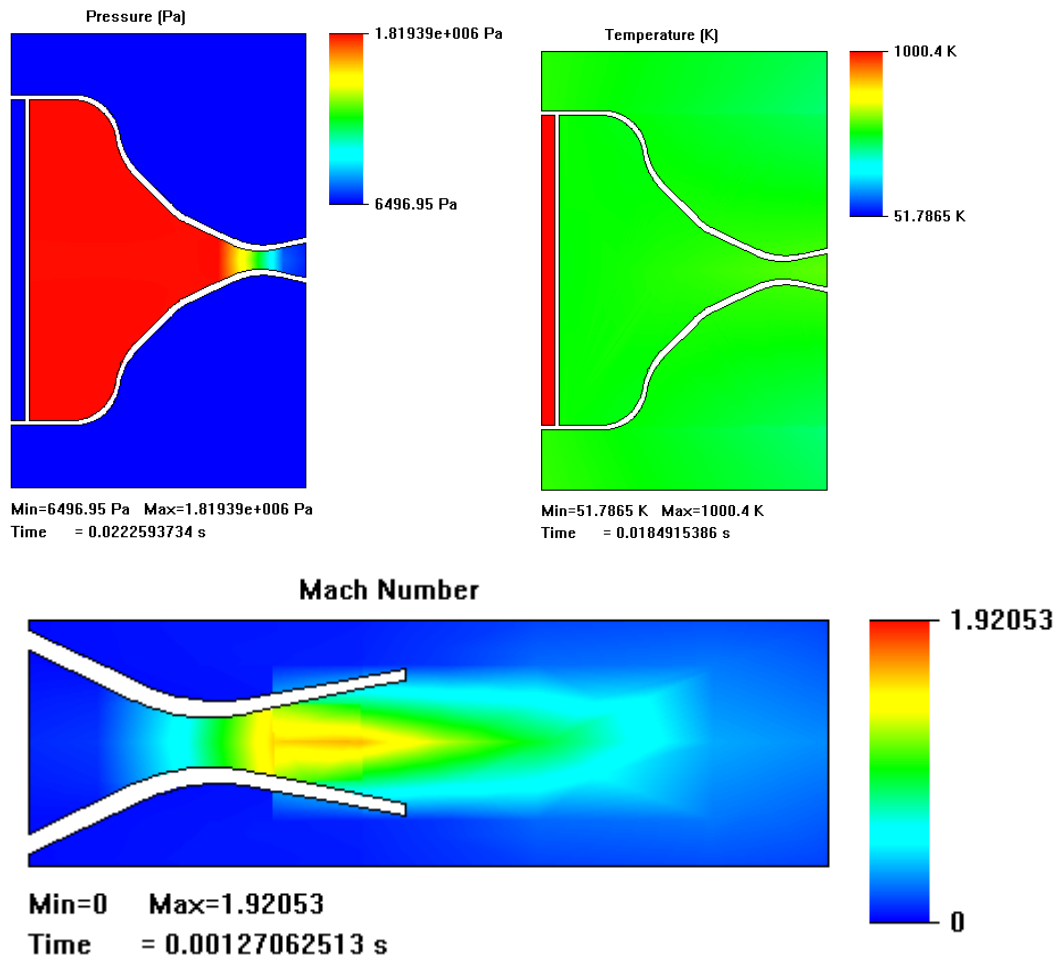


Figure 16 – CFDs for pressure, temperature and Mach number velocity

CHAPTER 4. ENGINE TEST

In this chapter oscillation modes and flutter are studied. Engine tests will be done in order to compare the results with the simulations. Because of the difficulty to calculate pressure or temperature inside the engine, a photo camera will be used. Then, some events will be compared with time.

4.1 Flutter test

High pressures, shockwaves and the elasticity of the materials produce vibrations in the structure of the rockets. These oscillation modes could enter into resonance with rocket body and it could be catastrophic. It could deform the structure and destroy it as happened with the firsts Saturn V. Apollo 6 that was launched by a Saturn V launch vehicle, for instance, had serious problems with resonances in a pipeline and it caused an engine failure. So flutter is a phenomenon to be considered.

Combustion could create undesired instabilities. Pressure in combustion chamber often varies and this was the reason that caused the failure of second stage engines of the first versions of Titan II missiles. These oscillations were of 0,1 Bar at 25 kHz.

4.2 Oscillation modes

Rocket body could come into resonance due to combustion. The air flowing in the combustion chamber creates a periodic force and if its vibration period is close to the natural frequency of the structure, it begins to deform. This force can create an important vibration of the body of the rocket and could destroy it.

In the following sections early tests will be shown. Some tests done by Clarissa Yuan related with flutter in the structure will be explained. Then, some simulations will be carried out with software in order to calculate the frequencies which could create flutter in the rocket structure.

4.2.1 Early tests

In this section early tests will be studied. Clarissa Yuan in her master thesis made two practical tests in order to investigate the frequency response of the second stage launcher. The first one was made in a wind tunnel and the second one was a real launch test.

As said before, the first test was done in a wind tunnel. The second stage launcher was introduced in it. Here, Angle of Attack (AoA) and wind speed can be changed. Accelerometers were put inside the payload fairing to calculate the vibrations of the body. It was excited with two speakers producing frequencies from 10 Hz to 800 Hz. The results of this test were not useful because later on it was discovered that the smaller size of the structure the higher frequency response it will have. See a Youtube video:

<http://www.youtube.com/watch?v=tmtl-cp0FUc>.

The second test was a real launch test and it was intended to be launched as the WikiSat team. See a Youtube Video:

<http://www.youtube.com/watch?v=264hK51WcXk>.

First of all, the Wiki-launcher is ignited inside the balloon from a launching ramp. Unfortunately there was water condensation in the nozzle that reacted with the propellant and it failed during the ignition. After a time to let the propellant dry it was decided to ignite the rocket in a tube at sea level without helium. The structure only achieved 20 m and the parachute failed but it was important to find out that some data was acquired during a real flight. It was possible to see the vibrations due to the burnout and the impact with the ground.

4.2.2 *Oscillation modes*

In this section some simulations are done with software **ANSYS 13.0**. A detailed model of the combustion chamber and nozzle was introduced in the program. Also, some initial conditions like environmental temperature and the propellant mass were introduced. Nozzle was set at 500 K and progressive gradient until the end that was set at 295.17 K. The aim was to calculate the natural frequencies of the body in order to see when the structure can enter into resonance and deformation.

Nine modes of natural frequencies were calculated as showed in the annexes. The first six were ignored because they correspond to the first six degrees of freedom and structure is in the air. There is no response in these modes, only when the structure is attached to a point that is not the case. Modes 7, 8, 9 and its natural frequencies are presented that are combination between the previous six modes. Tensions and deformations were calculated. In the figure 17, deformations for the three oscillation modes are shown.

So the frequencies in which the launcher could enter into resonance are 1512.1 Hz, 1604.5 Hz and 3052.8 Hz. This fact confirms the results of the test carried out in the wind tunnel. The natural frequencies of the structure are above 1 kHz and the frequency sweep of the speakers was from 10 Hz to 800 Hz. Real burn tests sensors showed that working frequencies are under 1kHz.

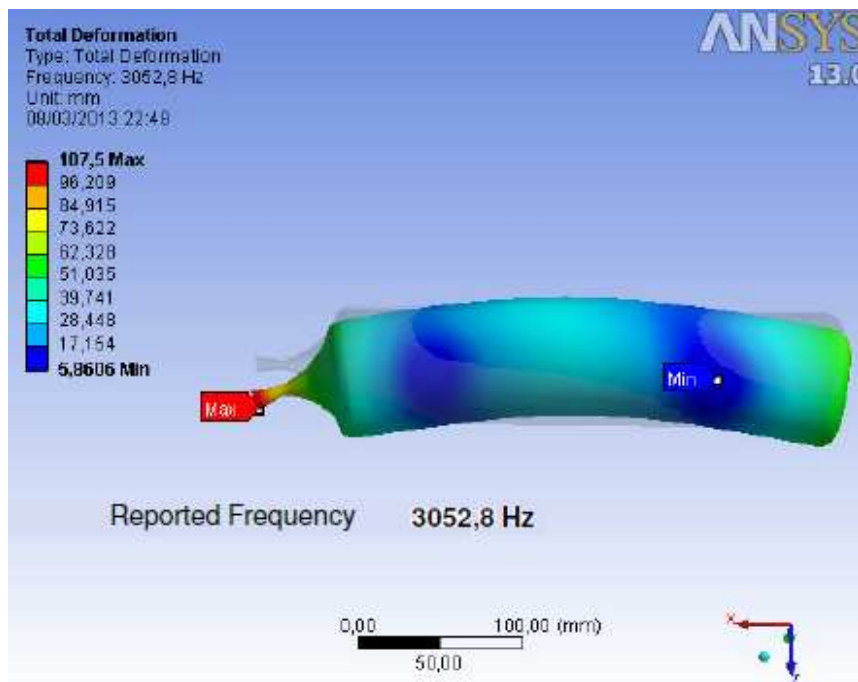
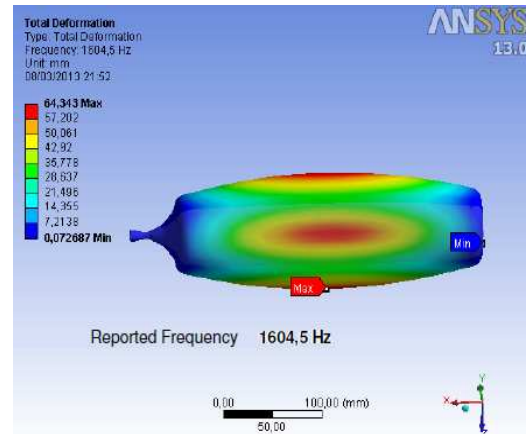
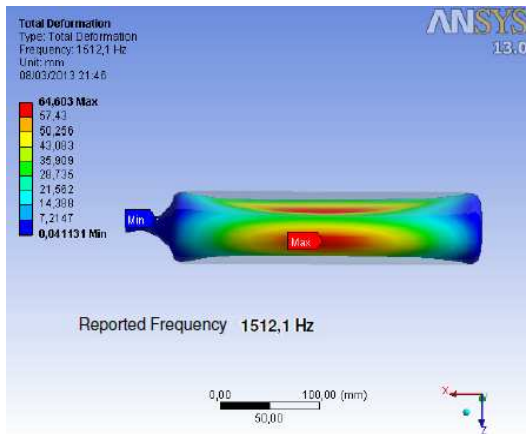
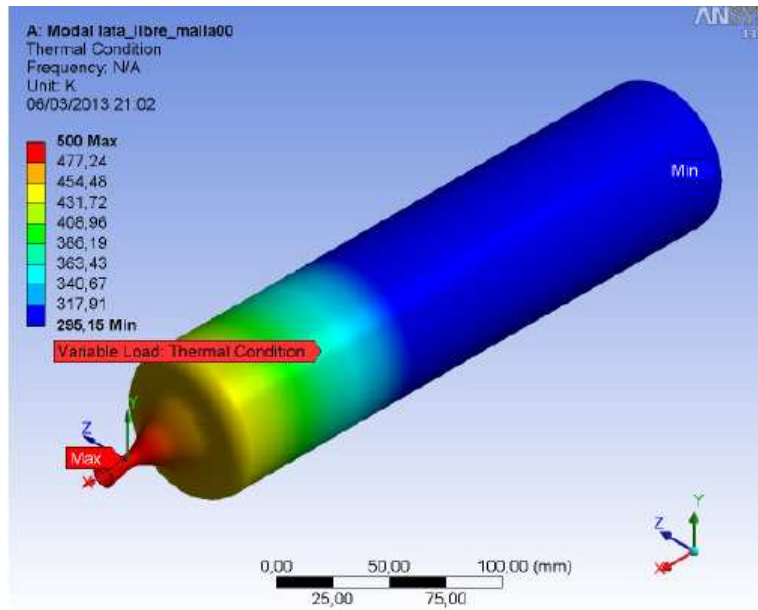


Figure 17 – Preheating and oscillation modes number 7, 8 and 9

4.3 Stage1 Burn03rd Test

The Stage1 Burn03rd test was started on July 27th, 2012 and burned on January 27th, 2013. We have to wait 6 month until safe conditions were achieved and a collaborating agreement with a quarry was obtained.

4.3.1 Test 03 setup

This burn is based on C1 propellant inside a 930 cc Argon welding bottle. The nozzle was a 4 mm throat attached with only 9 bolts of M2.

4.3.2 Results

The nozzle was ejected during the explosion as seen in figure 18. Initial hypothesis was too much powder in the ignition. Later we saw that the problem was the lack of ablative material between the bottle metal and the propellant grain.



Figure 18 – Stage1 Burn03rd pictures

This was our first burn in the quarry. The placement resulted very safe even the huge explosion. People were in safe conditions during all the test. A report was published in WikiSat YouTube channel here:

<http://www.youtube.com/watch?v=sPDQE7tLEQ0>

4.4 Stage1 Burn04th Test

The Stage1 Burn04th test was started on February 25th, 2013 and burned on March 03rd, 2013 but ignition failed. Second attempt was performed on March 10th, 2013.

4.4.1 Test 04 setup

This is a burn based on a C1 propellant inside a 930 cc Argon welding bottle and a steel nozzle with bolt seal. Bottle pressure was released. A small hole was performed in order to ensure the pressure is down and empty from Argon. Mixture was done inside the bottle. Upper bulkhead was cleaned with acetone. Propellant upper surface was flattened. The igniter was placed in the center of this surface. The engine was closed by eleven M3 bolts with a fiberglass and epoxy seal.

4.4.2 Results

The igniter failed in the first attempt. A relievable igniter was developed and the stage was burned in a second attempt. The stage burned very slow without a supersonic flame except for a moment as seen in figure 19. During this sudden increase of pressure the seal failed. Epoxy should be avoided in this seal. The propellant mixture process was bad. In future mixing procedures, a premix will be done in a cup. Since the burn time was 421 seconds and propellant length was 216 mm, the burn rate at a low pressure was set initially at 0.51 mm that is very slow compared to 6 mm/s that APCP composite propellant has. Thanks to this parameter, **Moon2.0** propellant burn calculations were corrected.



Figure 19 – Stage1 Burn04th pictures

A report was published in WikiSat YouTube channel here:
<http://www.youtube.com/watch?v=50vRoOJKgeY>

4.5 Stage1 Burn05th Test

The Stage1 Burn05th test was started on March 12th, 2013 and burned on March 24th, 2013 but ignition failed. Second attempt was performed on April 04th, 2013.

4.5.1 Test 05 setup

This is a burn based on a C2 propellant inside a 930 cc Argon welding bottle and a 4 mm throat steel nozzle with bold seal. Bottle flange was polished as well as the nozzle flange. The closure will be through 27 bolts M2x17 mm and nuts without no gasket or joint hoping that closure will be tightness and no pressure leak at this point. Propellant will be premixed in a cup adding 170Ap and 60St. We needed 6 cup but there is room for extra propellant if bolts were installed before filling the bottle. Next time, consider to install an protect bolts before filling.

4.5.2 Results

Due to the ignition failed in the first attempt and ablative material was not added at this time, we decided to do not use the nozzle and reuse it in the Burn08th as seen in figure 20. Since the burn time was 383 seconds and propellant length was 208 mm, the burn rate for the C2 propellant at low pressure was set at 0.54 mm/s that is higher than C1 burn rate as expected. Thanks to this parameter **Moon2.0** propellant burn calculations were corrected.



Figure 20 – Stage1 Burn05th pictures

The ablative problem is only seen if nozzle is present.. The ignition used was a reliable one so ignition confidence is increasing every attempt. A report was published in WikiSat YouTube channel here:

http://www.youtube.com/watch?v=XHli4xr_ytl

4.6 Stage1 Burn06th Test

The Stage1 Burn06th test was started on March 19th, 2013 and burned on March 24th, 2013. The manufacturer time and test time was reduced to only one week.

4.6.1 Test 06 setup

In this burn we are putting 4 mm throat nozzle to the limit with higher flow, larger burn time and a hotter/abrasive propellant which is the C2. This is a burn based on a 930 cc Argon welding bottle and a steel nozzle of 4 mm throat with bolted metallic seal. Bottle flange (46 mm of nominal diameter) was polished as well as the nozzle flange. The closure was done through 27 bolts M2x17 mm and nuts. C2 propellant was premixed in seven cups. Last cup was C1 propellant, without aluminum, to ensure a good slow propellant start. Bolts were installed before filling the bottle so higher volume was filled with APCP this time. Igniter has been normalized but this is the first real test for this kind of igniters.

4.6.2 Results

The nozzle was ejected during the explosion but supersonic flame was achieved for a moment before the explosion as seen in figure 21. We realized that, even the nozzle was attached by 27 bolts, the pressure increases anyway so the problem is not the ignition, is the lack of ablative material between the bottle metal and the propellant grain.



Figure 21 – Stage1 Burn06th pictures

The huge explosion was recorded by our slow motion camera. A report was published in WikiSat YouTube channel here:

<http://www.youtube.com/watch?v=xIRSAT0ghlo>

4.7 Stage1 Burn07th Test

The Stage1 Burn07th test was started on March 24th, 2013 and burned on March 27th, 2013. This is the faster test we have done up to now from the beginning of manufacturing until a succeeded burn and report only in 3 days.

4.7.1 Test 07 setup

This is a burn based on C2 propellant inside a 930 cc Argon welding bottle and a 9 mm throat steel nozzle with bold seal and no joint. In order to avoid the explosion, an ablative layer was attached to the bottle interior walls. Igniter worked for the second time. Metallic seal remains closed.

4.7.2 Results

Moon2.0 burn editor simulation said 64 seconds of burn time while real burn was between 60 and 80 seconds. Flame was not supersonic as seen in figure 22 where pressure was not high enough.



Figure 22 – Stage1 Burn07th pictures

Next burn can have the 4 mm throat because looks like the explosion problem was fixed. A report was published in WikiSat YouTube channel here:

<http://www.youtube.com/watch?v=xg5LbAJ94K4>

4.8 Stage1 Burn08th Test

The Stage1 Burn08th test was started on April 02nd 2013, first try was on April 07th, 2013 and finally burned on April 21th, 2013. The 4 mm nozzle was tested with a bore burner.

4.8.1 Test 08 setup

This burn is based on C2 propellant inside a 930 cc Argon welding bottle and a 4 mm throat steel nozzle with bold seal and no joint. Ablative material was applied and bolts were placed before propellant insertion. Igniter was the same as previous burns. First try was a single igniter. Second attempt we installed

two igniters. It worked, but second igniter blocked the throat and provoked the explosion.

4.8.2 Results

In the first attempt ignition failed, powder was loosed during tight nuts. In the second attempt, the nozzle was ejected during the explosion as seen in figure 23. Looks like second igniter block the throat and nozzle was ejected. Bolts are too weak. M3 mm bolts should be used instead of M2 mm bolts.



Figure 23 – Stage1 Burn08th pictures

This burn should be repeated but using stronger bolts. A report was published in WikiSat YouTube channel here:

<http://www.youtube.com/watch?v=Ok4caEWjMGU>

4.9 Stage1 Burn09rd Test

The Stage1 Burn09th test was started on April 07th, 2013 and burned on April 14th, 2013. This burn was dedicated to test a Core burner instead a Bore burner.

4.9.1 Test 09 setup

This is one of the development prototypes for the stage1 rocket of the WikiLauncher. It is a burn based on C1 propellant inside a 930 cc Argon welding bottle and a 9 mm throat steel nozzle, core burn and 6 mm drill, with bolted seal and ablative material between metal and propellant. Igniter is the same as previous burn but positioned at the final moment. Looks like vibrations during tight nuts made these igniters fail as happened in Burn05th and Burn08th.

4.9.2 Results

Pressure increased slowly and exploded after 25 seconds. Flame was under expanded before the rapid explosion and weak during the burn. As seen in figure 24, looks like the propellant supported the pressure, fractured and then exploded because metallic fragments of the bottle were small. Nozzle required a 22 mm exhaust diameter instead of 26 mm of the used nozzle.




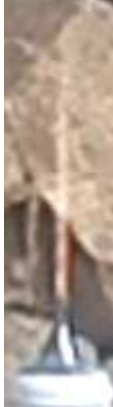

Figure 24 – Stage1 Burn09th pictures

The test could be repeated with an adapted nozzle but looks like Core burner has too much pressure to be supported by the propellant then soft propellants should be developed. A report was published in WikiSat YouTube channel here: <http://www.youtube.com/watch?v=cS1yJ17QyeE>

4.10 Stage1 Burn tests summary

Following, table 6 is a summary of the main results for the seven burn tests performed during this work.

Table 6 - Summary for stage1 burn tests

Burn test number	03rd	04th	05th	06th	07th	08th	09th
Development (Days)	180	7	27	5	3	5	7
Burned date (2013)	27/Jan	10/Mar	07/Apr	24/Mar	10/Mar	21/Apr	14/Apr
Propellant used	C1	C1	C2	C2	C2	C2	C1
Propellant mass [grams]	1364	1380	1330	1445	210	1405	1414
Dry mass [grams]	1152	1215	1200	1167	1254	1207	1234
Propellant mass fraction	54.2%	53.2%	53.8%	55.3%	14.3%	53.8%	53.4%
Burner type	Bore	Bore	Bore	Bore	Bore	Bore	Core
Burn time [seconds]	1	421	383	14	80	10	25
Nozzle throat [mm]	4	9	4	4	9	4	9
Nozzle bolt [mm] / Qty.	2x9	3x9	2x27	2x27	3x18	2x27	3x18
Ended Burned/Exploded	Explod	Burned	Burned	Explod	Burned	Explod	Explod
Supersonic flame	No		No		No		No

CHAPTER 5. CONCLUSIONS

Related to the propulsion issues, this work has more real burn tests than the previous works in such a way that calculations could be compare with real data.

5.1 Conclusions

Following, main conclusions are presented:

- Pressure tests were performed for the Soda Can where maximum pressure was set at 18 Bar. This structure will be used in the WikiLauncher second stage with a 4 mm throat nozzle thanks to the high propellant mass fraction about 80%. Bore burner will be used due to the constant working pressure allows to work near the pressure limit.
- It was decided to carry out the rest of tests using an Argon bottle due to its higher size and tolerance in pressure. The reason was to focus the experimentation in the flow results and thermal loads, and not to be aware about maximum pressure.
- Tests that were carried out with Argon bottle showed how APCP propellant behaves inside a container with both, 9 mm and 4 mm throat nozzle, before continuing with Soda Can study.
- Argon bottle was tested under thermal load conditions that could be used in the WikiLauncher fist stage but propellant mass fraction should be improved because it is still worse than amateur rocket engines.
- Despite the large amount of experimental tests with the first stage, it is not possible to determine if the design will tolerate the thermal load during the burn.
- It was proven that the 4 mm throat nozzle cannot be attached to the bottle only with M2 bolts even twenty seven bolts are used. M3 bolts are recommended, nine bolts are enough but eighteen are best.
- The 4 mm nozzle has problems with loosed objects larger than 4 mm in diameter because the bottle can explode.
- The Stage1 Burn09th has proven that a Core Burner has a too fast pressure growth and propellant is not able to resist such a pressure, cracking and exploding suddenly.
- Frequency modal study for the Argon bottle demonstrates that natural frequencies are in the range of kilohertz far from the working ranges as recorded by the sensors.

5.2 Future work

The future study should be focused on to achieve a propellant mass fraction higher than 70%.

Although many real burns were done, some of them should be repeated because of the often explosions. Stage1 Burn08th exploded so it should be done another time. This test will determine the burning time. This value will give us the burn rate to calibrate the simulations as we did with Argon bottle.

Frequency modal and thermal load tests should be done for the Soda Can structure as well.

5.3 Environmental impact

When a launching has been performed, the satellite is in orbit two weeks approximately. Then, the satellite reenters to the atmosphere and it is burnt, without leaving any residue. The rocket falls on the Earth surface, usually on the sea, and it can be recovered.

In the long term, if satellites are put in orbit using small rockets as WikiLauncher, the environmental impact is considerably reduced.

On the other hand, the use of solid propellant is more polluting than the use of liquid propellant, but we must take into account that in case of catastrophic failure, liquid propellant burns and in solid propellant the fire is instantaneously extinguished.

Furthermore, if launchings are performed near the sea, the chances of possible damages are reduced, and the risks of damaging people is really low, due to the launching is performed in the stratosphere.

Engine test were performed in a stone quarry, far from population. While all the tests were performed, safety measures were taken into account to assure that nobody could be damaged during the project.

CHAPTER 6. BIBLIOGRAPHY

[1] Anderson, John D. Jr.; (January de 2001), *Fundamentals of Aerodynamics* (3rd Edition edición). McGraw-Hill Science/Engineering/Math. (1984) [ISBN 0-07-237335-0](#)

[2] Larson, R.; Wertz, J.; (Eds.), *Space Mission Analysis and Design*, Kluwer-Microcosm (1999)

ANNEXES

TÍTOL DEL TFC: Study of a Coke Can as a rocket structure and its flutter effects

TITULACIÓ: Enginyeria Tècnica Aeronàutica, especialitat Aeronavegació

AUTORS: Pau Manyà Saez i Daniel Gómez Sañé

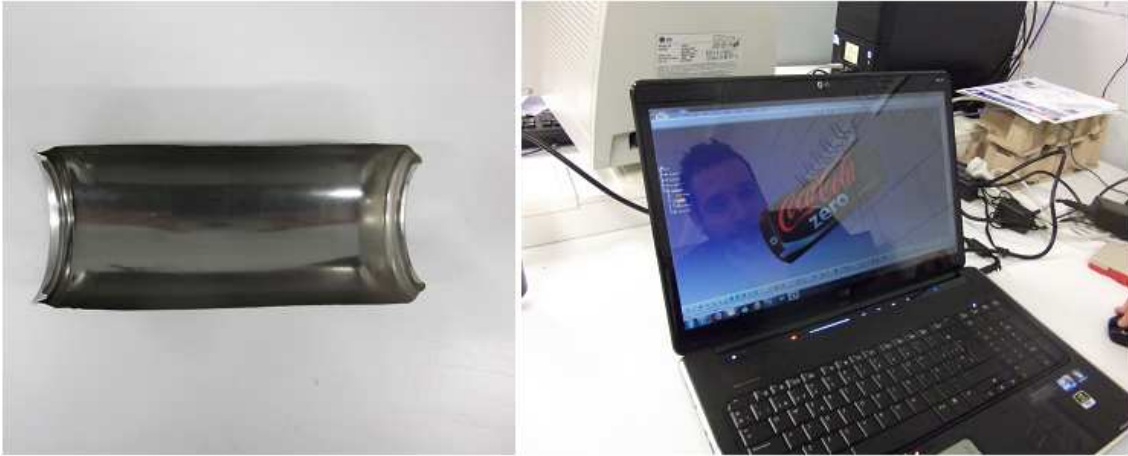
DIRECTOR: Joshua Tristancho Martínez

CODIRECTOR: Jordi Gutiérrez Cabello

DATA: 10 de Maig de 2013

Coke Can modeling (CATIA v5)

Modeling process thanks to Javier Sánchez Martínez



Inertial matrix by Catia v5

The screenshot shows the CATIA v5 software interface with the 'Measure Inertia' dialog box open. The dialog displays the following data:

Characteristics		Center Of Gravity (G)	
Volume	4,269e-006m3	Gx	0mm
Area	0,061m2	Gy	0mm
Mass	0,034kg	Gz	72,536mm
Density	7860kg_m3		

Inertia Matrix / G			
IxxG	1,097e-004kgm2	IyyG	1,097e-004kgm2
IyyG	0kgm2	IzzG	2,332e-003kgm2
IxxG	0kgm2	IyyG	0kgm2

Principal Moments / G			
M1	2,332e-003kgm2	M2	1,097e-004kgm2
M2	1,097e-004kgm2	M3	1,097e-004kgm2

Frequency modes for the Argon bottle

Elaborado por Jordi Tudela (e-mail: j_tudy@msn.com)

Objeto de estudio Depósito de combustible y tobera de expulsión de gases

Revisado por (UPC EETAC) Joshua Tristancho

Software empleado Pre-proceso, cálculo y post-proceso en Ansys Release 13.0
Fecha 08-03-2013

Cálculo de frecuencias propias o naturales en depósito de combustible y tobera de expulsión de gases. Geometría libre: sin restricciones, cargas, soportes o apoyos. Se añade peso de 1,98Kg correspondiente al combustible sólido empleado de densidad 1762Kg/m³ y CdG (-195.071,0,0). Temperatura ambiente exterior 295,15K. Temperatura en tobera 500K. Se elimina el tabique divisor intermedio heredado de la geometría inicial por su no funcionalidad mecánica. Se calculan los 9 primeros modos de frecuencias naturales, no siendo objeto de estudio los 6 primeros por su correspondencia con los 6 grados de libertad (sólido rígido libre). Se calculan las deformaciones y tensiones correspondientes a los modos 7, 8 y 9.

Especificaciones del análisis:

Object Name Pieza 1

Length X 358,76 mm

Length Y 72,6 mm

Length Z 72,6 mm

Volume 82855 mm³

Mass 0,65041 kg

Geometría y punto de masa

Object Name Point Mass

State Fully Defined

Scope

Coordinate System Global Coordinate System

Assignment Structural Steel

Nonlinear Effects Yes

Thermal Strain Effects Yes

X Coordinate -195,071 mm

Y Coordinate 0, mm

Z Coordinate 0, mm

Definition

Mass 1,98 kg

Behavior Deformable

Pinball Region All

Density 7.85e-006 kg mm⁻³

Coefficient of Thermal Expansion 1.2e-005 C⁻¹

Specific Heat 4.34e+005 mJ kg⁻¹ C⁻¹

Thermal Conductivity 6.05e-002 W mm⁻¹ C⁻¹

Resistivity 1.7e-004 ohm mm

Material

Compressive Ultimate Strength MPa: 0

Compressive Yield Strength MPa: 250

Tensile Ultimate Strength MPa: 460

Reference Temperature C: 22

Strength Coefficient MPa: 920

Strength Exponent: -0.106

Ductility Coefficient: 0.213

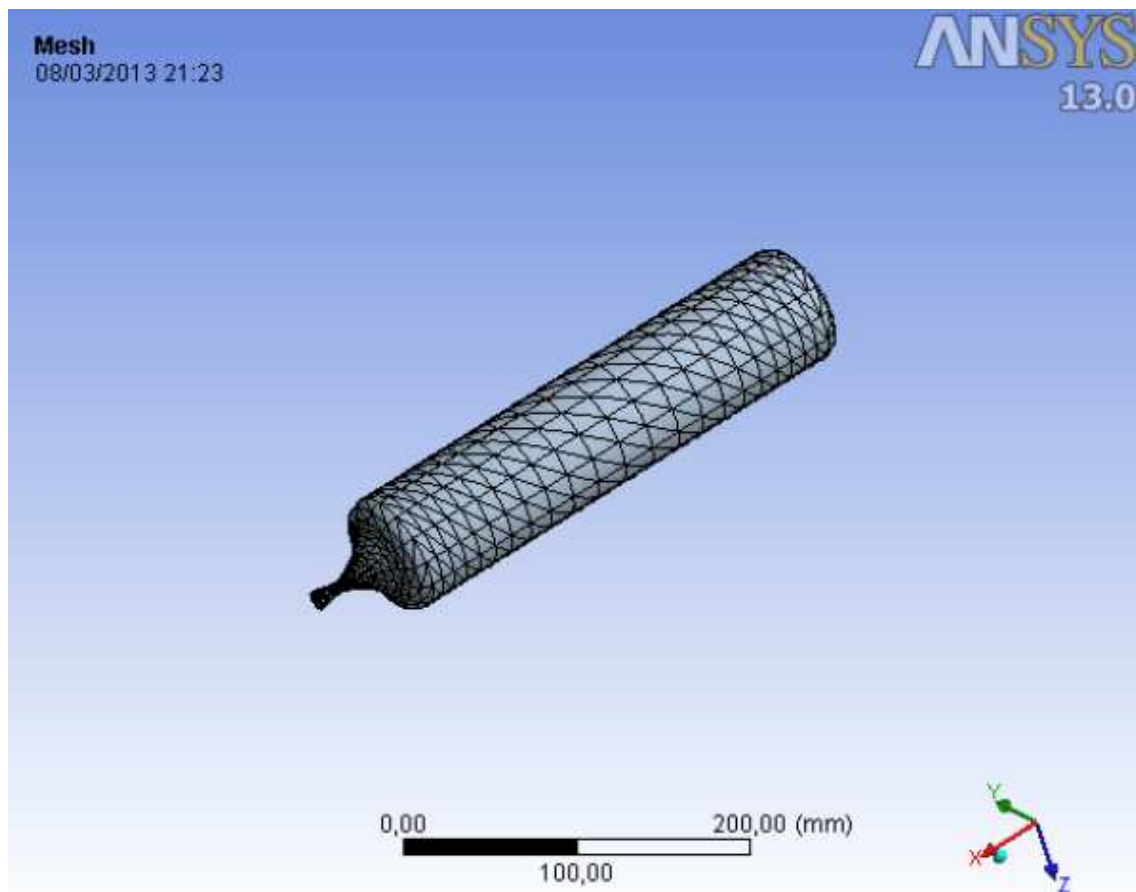
Ductility Exponent: -0.47

Cyclic Strength. Coefficient MPa: 1000

Cyclic Strain. Hardening Exponent: 0.2

Young's Modulus MPa: 200.000

Poisson's Ratio: 0.3



Object Name: Mesh

State: Solved

Defaults

Physics Preference: Mechanical

Relevance: 0

Sizing

Use Advanced Size

Function

On: Curvature

Relevance Center Medium

Initial Size Seed Active Assembly

Smoothing Medium

Transition Fast

Span Angle Center Medium

Curvature Normal Angle Default (45,0 °)

Min Size 0,08 mm

Max Face Size 20,0 mm

Max Size 20,0 mm

Growth Rate 1,1

Minimum Edge Length 0,544490 mm

Inflation

Use Automatic Inflation None

Inflation Option Smooth Transition

Transition Ratio 0,272

Maximum Layers 5

Growth Rate 1,2

Inflation Algorithm: Pre

View Advanced Options: No

Advanced

Shape Checking Standard Mechanical

Element Midside Nodes Program Controlled

Straight Sided Elements: No

Number of Retries: 0

Extra Retries For Assembly: Yes

Rigid Body Behavior Dimensionally Reduced

Mesh Morphing: Disabled

Defeaturing

Pinch Tolerance: Default (0,270 mm)

Defeaturing Tolerance: Default (0,150 mm)

Statistics

Nodes: 8971

Elements: 4499

Análisis Modal

Object Name Modal (A5)

State Solved

Definition

Physics Type Structural

Analysis Type Modal

Solver Target Mechanical APDL

Options

Environment Temperature 295,15 K

Generate Input Only No

Unit System Metric (mm, kg, N, s, mV, mA) Degrees rad/s Kelvin

Angle Degrees

Rotational Velocity rad/s

Temperature Kelvin

Object Name Analysis Settings

State Fully Defined

Options

Max Modes to Find 9

Limit Search to Range No

Solver Controls

Solver Type Program Controlled

Output Controls

Calculate Stress Yes

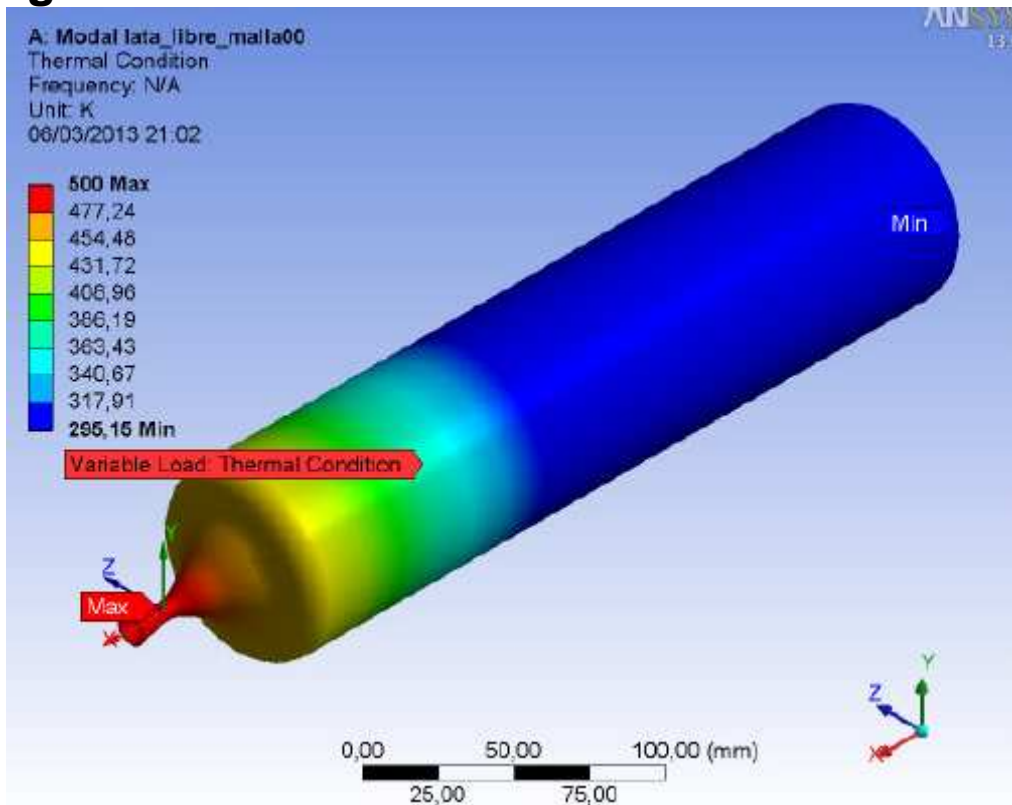
Calculate Strain Yes

Analysis Data Management

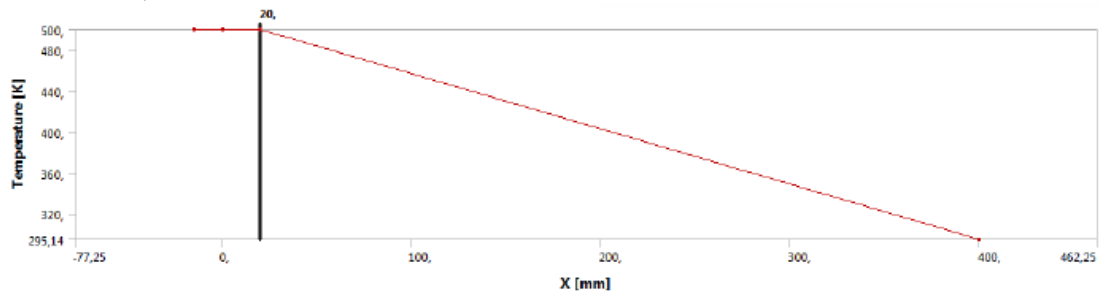
Solver Units Active System

Solver Unit System nmm

Cargas



Temperature of the body
 From -15 mm to 0 mm at 500 K,
 400 mm at 295,15 K



Object Name *Thermal Condition*
 State Fully Defined
 Scope
 Scoping Method Geometry Selection
 Geometry 1 Body
 Definition
 Type Thermal Condition
 Magnitude Tabular Data
 Suppressed No
 Tabular Data
 Independent Variable X
 Coordinate System Global Coordinate System

Deformaciones y tensiones Modo 7

Object Name *Total Deformation Equivalent (von-Mises) Stress*

State Solved

Scope

Scoping Method Geometry Selection

Geometry All Bodies

Definition

Type Total Deformation Equivalent (von-Mises) Stress

Mode 7,

Identifier

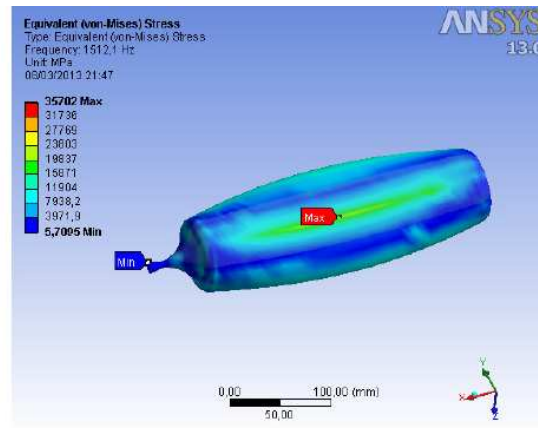
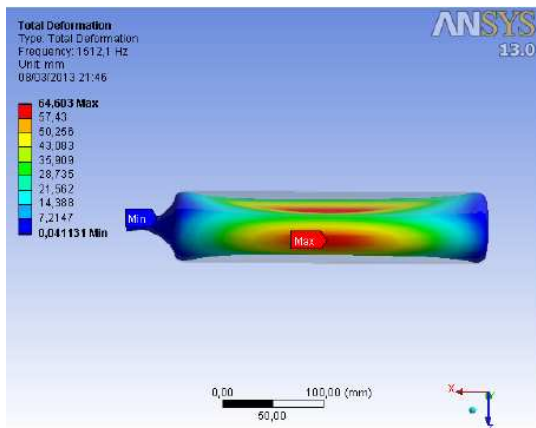
Results

Minimum 4,1131e-002 mm 5,7095 MPa

Maximum 64,603 mm 35702 MPa

Information

Reported Frequency 1512,1 Hz



Deformaciones y tensiones Modo 8

Object Name *Total Deformation Equivalent (von-Mises) Stress*

State Solved

Scope

Scoping Method Geometry Selection

Geometry All Bodies

Definition

Type Total Deformation Equivalent (von-Mises) Stress

Mode 8,

Identifier

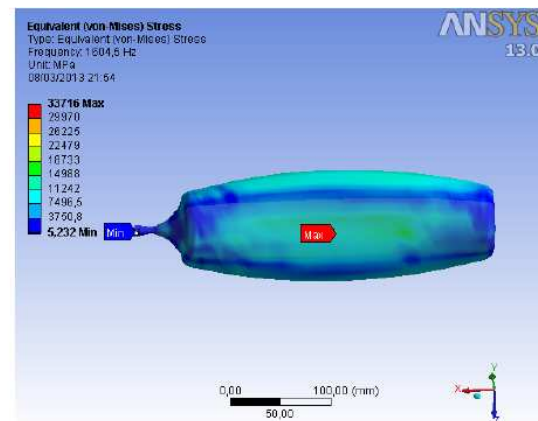
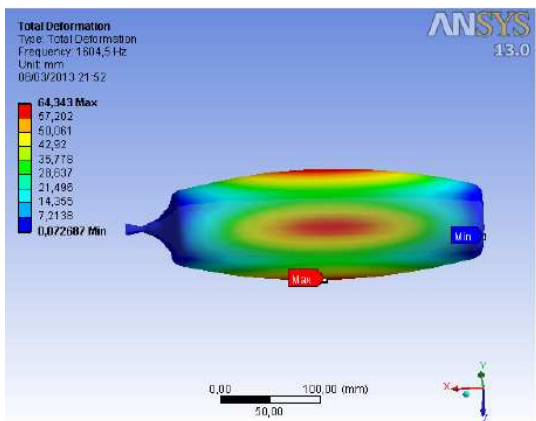
Results

Minimum 7,2687e-002 mm 5,232 MPa

Maximum 64,343 mm 33716 MPa

Information

Reported Frequency 1604,5 Hz



Deformaciones y tensiones Modo 9

Object Name *Total Deformation Equivalent (von-Mises) Stress*

State Solved

Scope

Scoping Method Geometry Selection

Geometry All Bodies

Definition

Type Total Deformation Equivalent (von-Mises) Stress

Mode 9,

Identifier

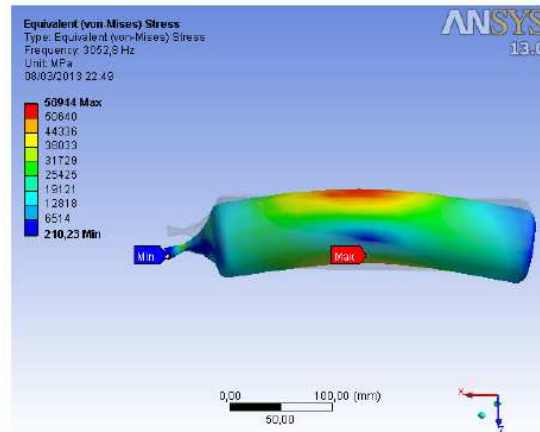
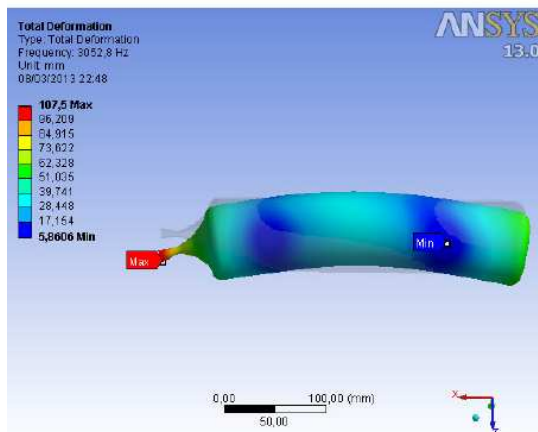
Results

Minimum 5,8606 mm 210,23 MPa

Maximum 107,5 mm 56944 MPa

Information

Reported Frequency **3052,8 Hz**



Conclusiones estudio modal

A la vista de los resultados obtenidos, las frecuencias críticas a tener en cuenta para evitar la entrada en resonancia en los correspondientes casos de excitación son;

1512,1 Hz

1604,5 Hz

3052,8 Hz

State Solved

Adaptive Mesh Refinement

Max Refinement Loops 1,

Refinement Depth 2

Modal summary

Modal	Frequency
Mode 1	3,6255e-003 Hz
Mode 2	5,2672e-003 Hz
Mode 3	6,914e-003 Hz
Mode 4	1,1235e-002 Hz
Mode 5	1,2338e-002 Hz
Mode 6	1,6031e-002 Hz
Mode 7	1512,1 Hz
Mode 8	1604,5 Hz
Mode 9	3052,8 Hz

Flow simulator module (SolidWorks)

INPUT DATA

Initial Mesh Settings

Automatic initial mesh: On
 Result resolution level: 2
 Advanced narrow channel refinement: Off
 Refinement in solid region: Off

Geometry Resolution

Evaluation of minimum gap size: Automatic
 Evaluation of minimum wall thickness: Automatic

Computational Domain

Size

X min	-0.070 m
X max	0.070 m
Y min	-0.030 m
Y max	0.030 m
Z min	-0.030 m
Z max	0.030 m

Boundary Conditions

2D plane flow	None
At X min	Default
At X max	Default
At Y min	Default
At Y max	Default
At Z min	Default
At Z max	Default

Physical Features

Heat conduction in solids: Off
 Time dependent: On
 Gravitational effects: Off
 Flow type: Laminar and turbulent
 High Mach number flow: On
 Default roughness: 0 micrometer
 Default wall conditions: Adiabatic wall

Ambient Conditions

Thermodynamic parameters	Static Pressure: 10132.00 Pa Temperature: 293.20 K
Velocity parameters	Velocity vector Velocity in X direction: 0 m/s

	Velocity in Y direction: 0 m/s Velocity in Z direction: 0 m/s
Turbulence parameters	Turbulence intensity and length Intensity: 0.10 % Length: 7.260e-004 m

Material Settings

Fluids

Air

Boundary Conditions

Inlet Mass Flow 1

Type	Inlet Mass Flow
Faces	Face<0>@Revolución2
Coordinate system	Face Coordinate System
Reference axis	X
Flow parameters	Flow vectors direction: Normal to face Mass flow rate normal to face: 0.0070 kg/s Inlet profile: 0
Thermodynamic parameters	Approximate pressure: 3343725.00 Pa Static pressure: 10132.00 Pa Temperature: 2790.00 K
Turbulence parameters	Turbulence intensity and length Intensity: 0.10 % Length: 7.260e-004 m
Boundary layer parameters	Boundary layer type: Turbulent

Calculation Control Options

Finish Conditions

Finish conditions	If one is satisfied
Maximum physical time	1.000 s

Solver Refinement

Refinement: Disabled

Results Saving

Save before refinement	On
------------------------	----

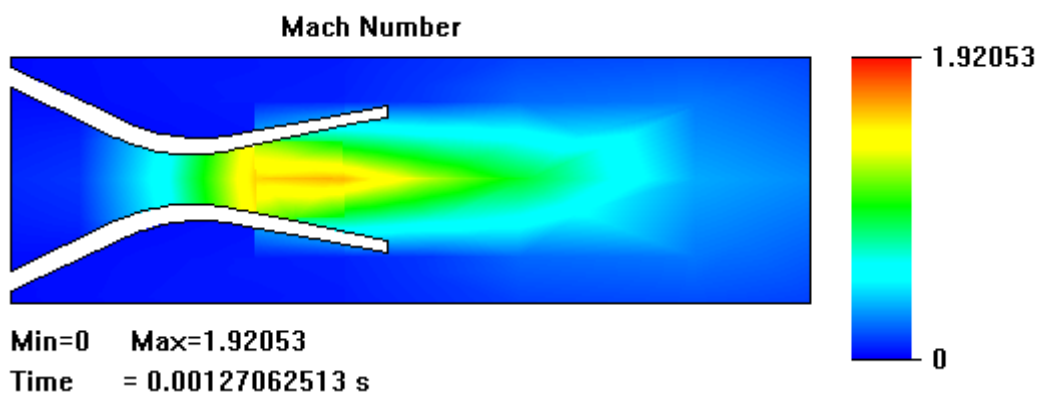
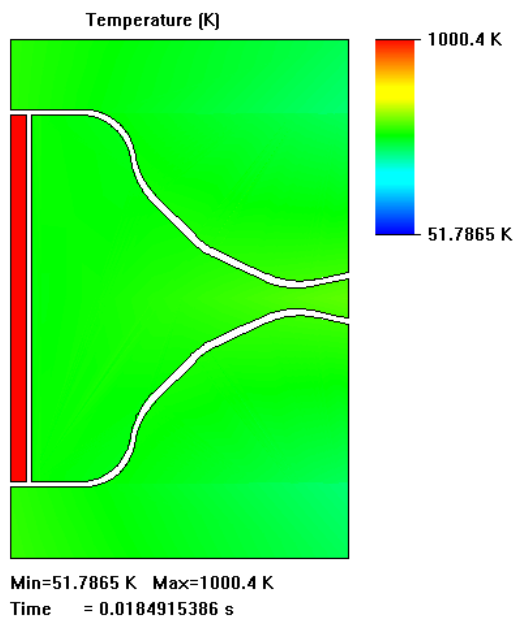
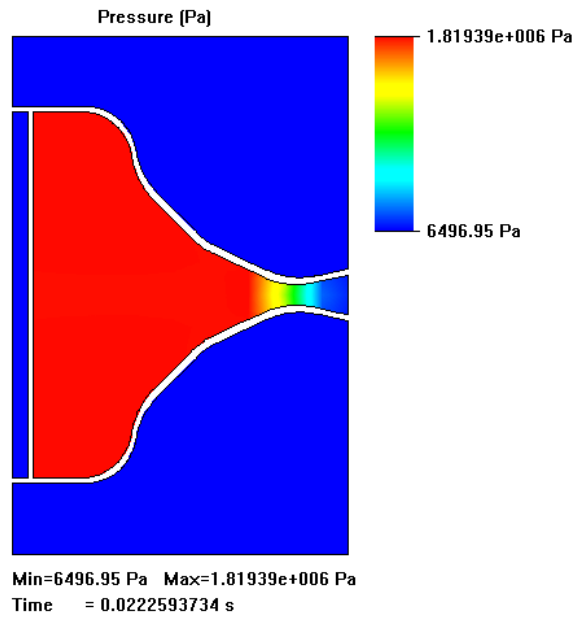
Advanced Control Options

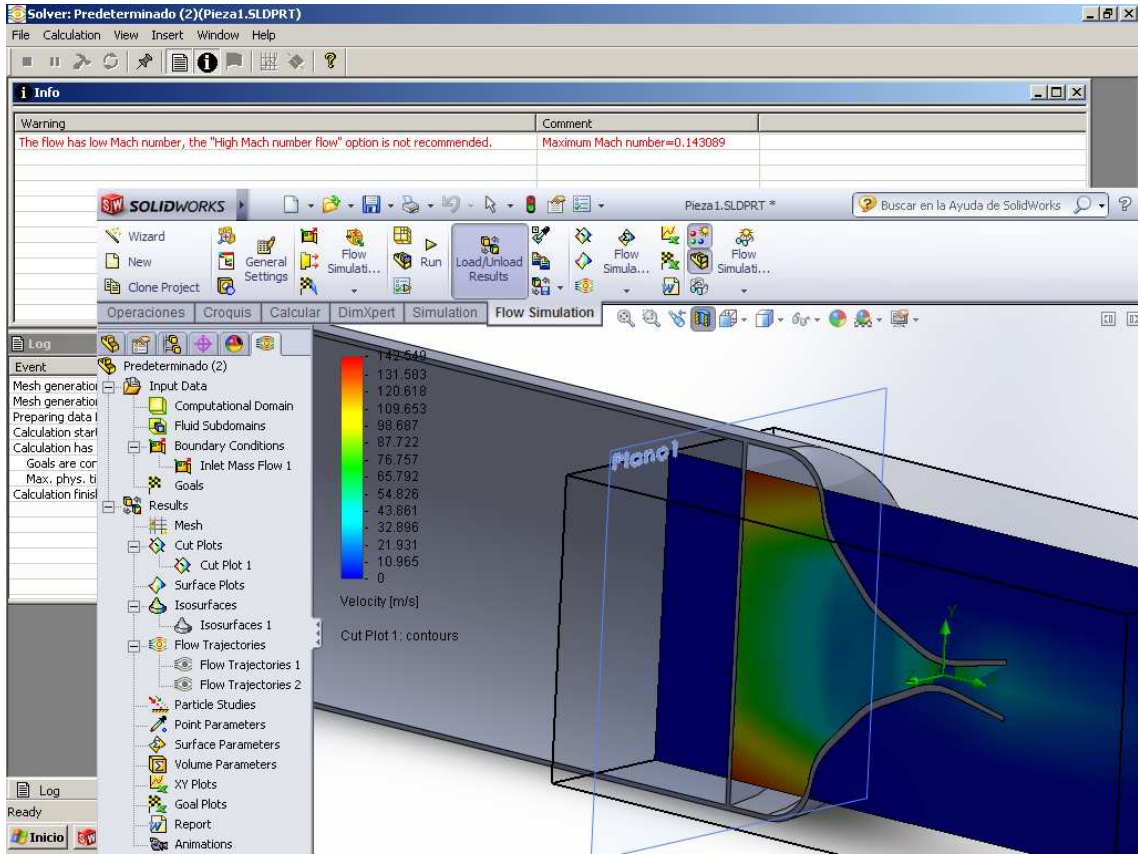
Flow Freezing

Flow freezing strategy	Disabled
------------------------	----------

Manual time step (Freezing): Off

Manual time step: Off

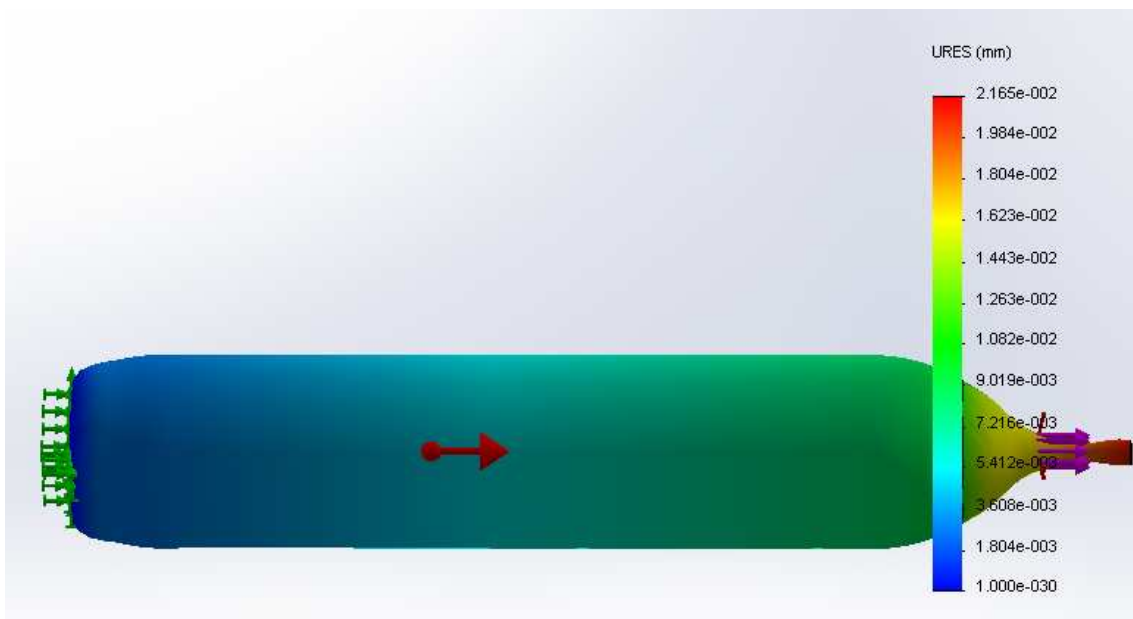




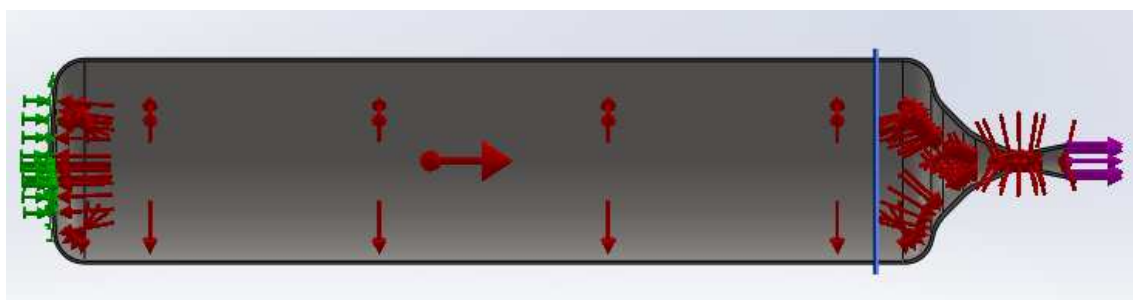
SolidWorks deformation study due to thrust and pressure



Intuitive vision of the relative bottle deformation



Deformation



Forces (1000 Nw) and pressures (165 Bar)

Nombre de modelo: Piezadani
Nombre de estudio: Estudio 1
Tipo de resultado: Deformación unitaria estática Deformaciones unitarias1
Escala de deformación: 1659.4



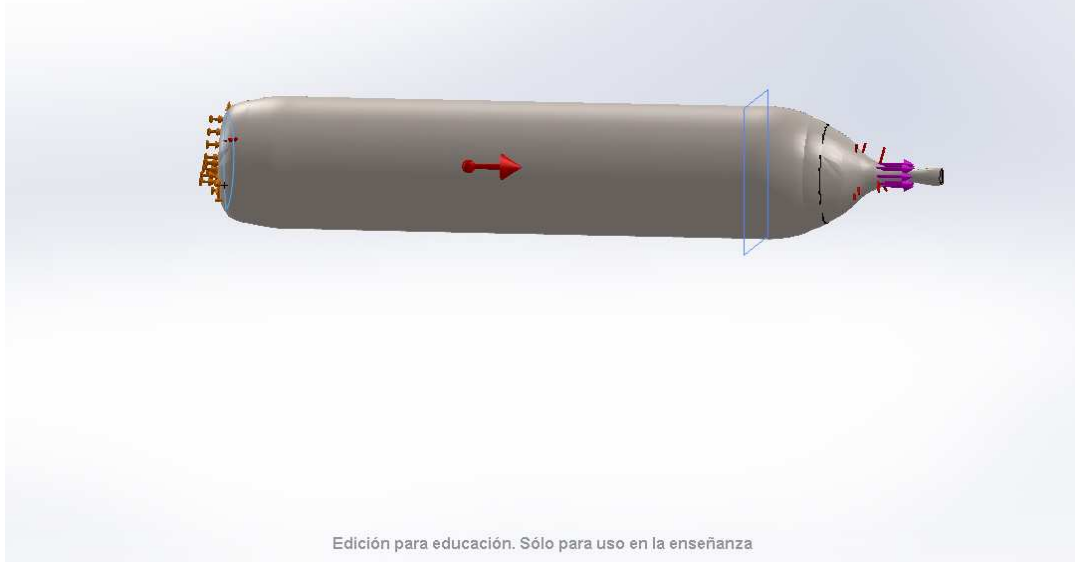
Unitary deformation

Nombre de modelo: Piezadani
Nombre de estudio: Estudio 1
Tipo de resultado: Desplazamiento estático Desplazamientos1
Escala de deformación: 1659.4



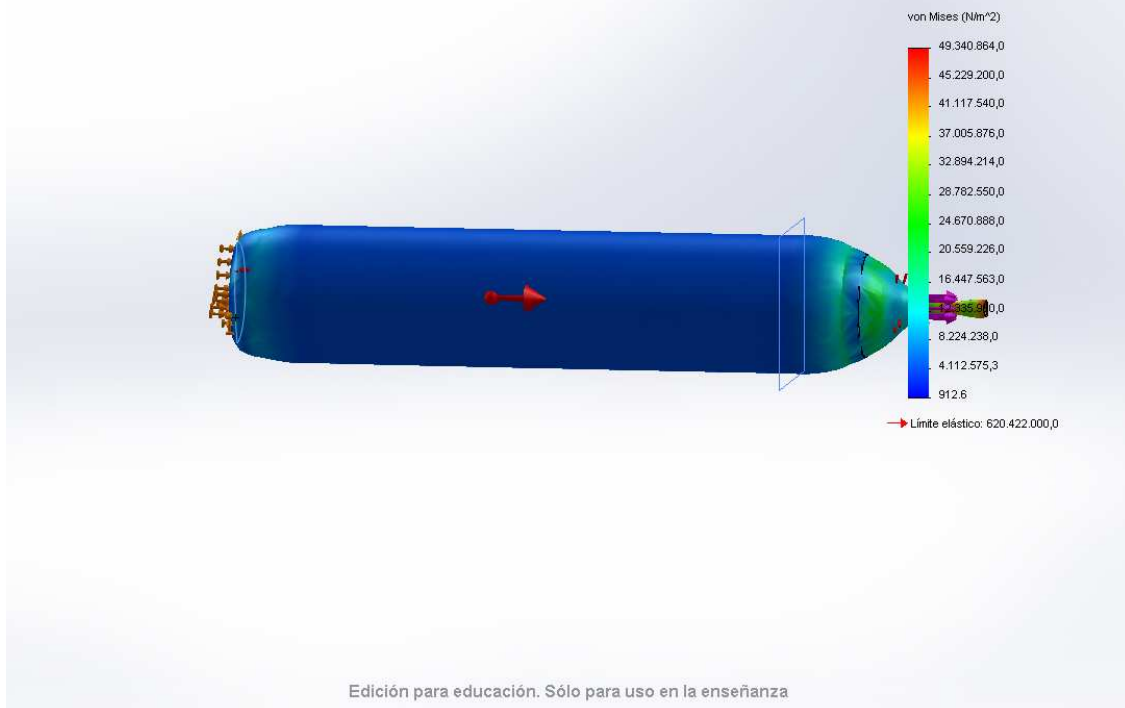
Displacement with scale

Nombre de modelo: Piezadani
Nombre de estudio: Estudio 1
Tipo de resultado: Forma deformada Desplazamientos(1)
Escala de deformación: 1659,4



Displacement

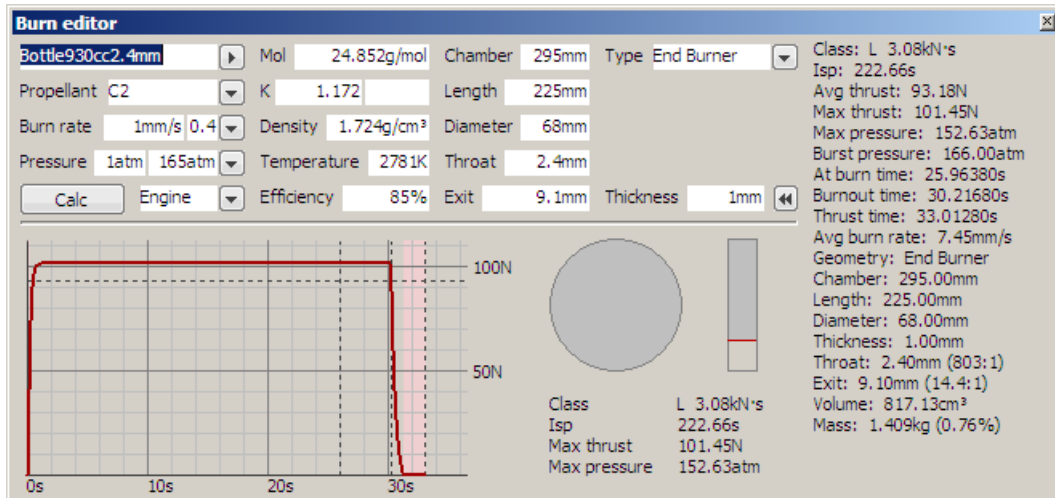
Nombre de modelo: Piezadani
Nombre de estudio: Estudio 1
Tipo de resultado: Static tensión nodal Tensiones1
Escala de deformación: 1659,4



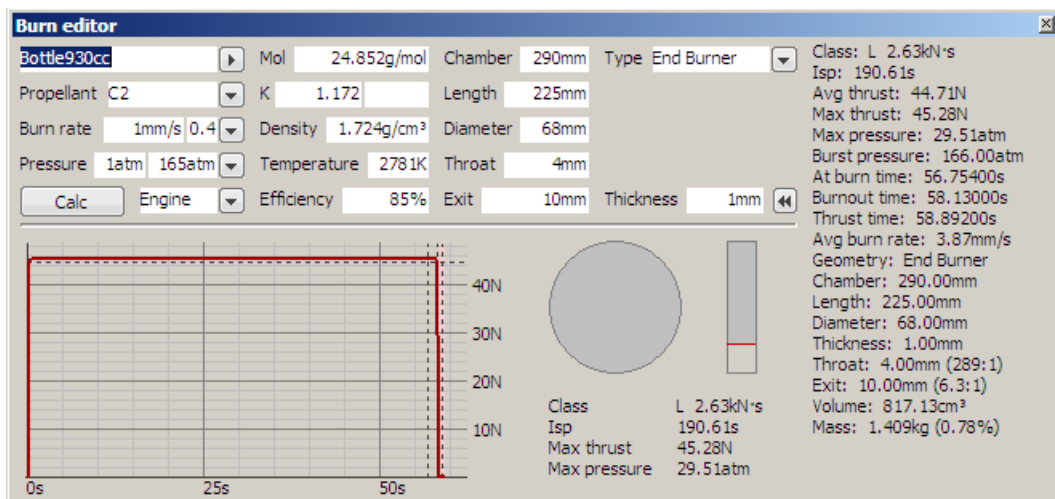
Tensions

2.4 mm and 4 mm throat propellant burn series of Moon2.0 simulations

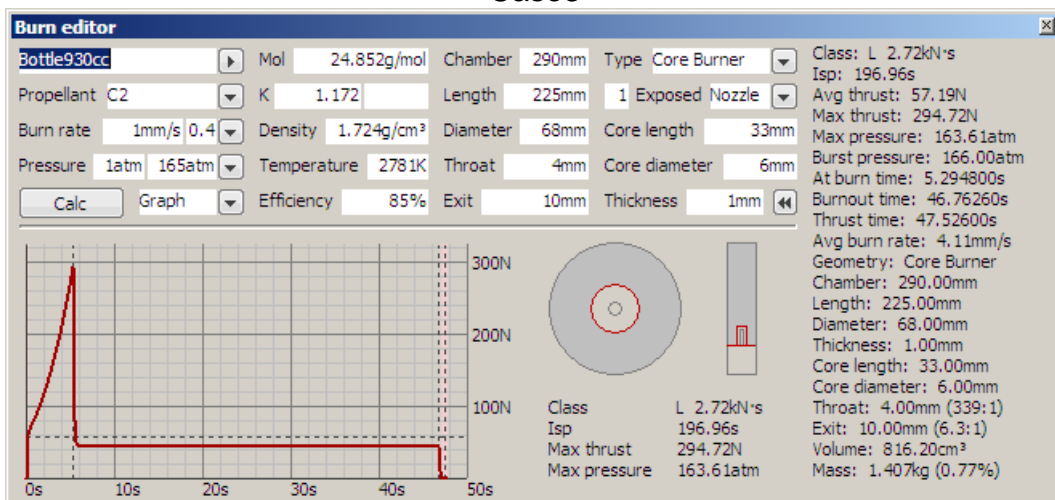
Case1



Case2

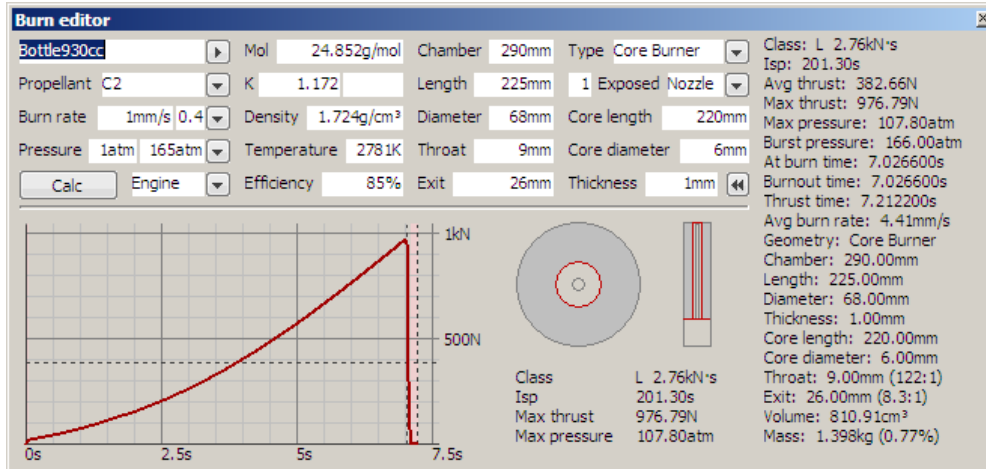


Case3

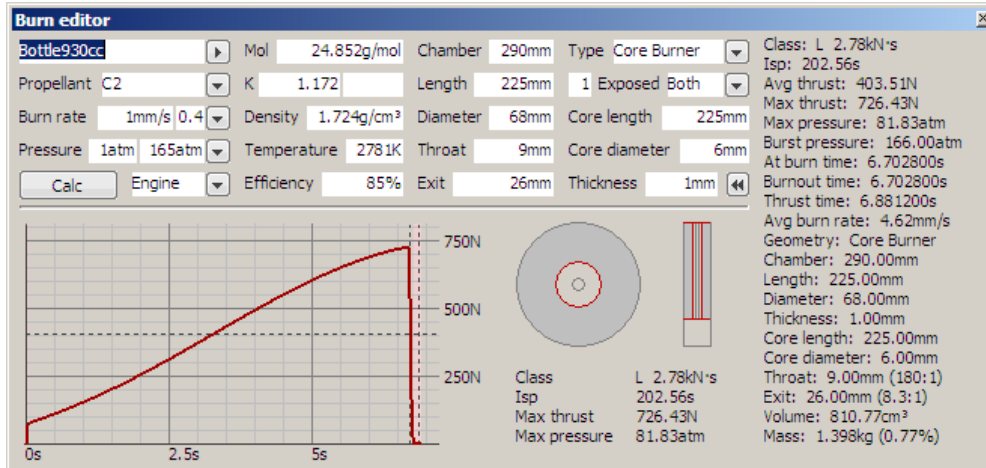


9 mm throat propellant burn series of Moon2.0 simulations

Case4



Case5



Case6

